Effects of dissipation on solitons in the hydrodynamic regime of graphene

Thomas Zdyrski and John McGreevy
University of California San Diego, La Jolla, California 92093, USA

(Received 17 April 2019; revised manuscript received 12 June 2019; published 28 June 2019)

We use hydrodynamic techniques to analyze the one-dimensional propagation of solitons in gated graphene on an arbitrary uniform background current. Results are derived for both the Fermi liquid and Dirac fluid regimes. We find that these solutions satisfy the Korteweg–de Vries–Burgers equation. Viscous dissipation and Ohmic heating are included, causing the solitons to decay. Experiments are proposed to measure this decay and thereby quantify the shear viscosity in graphene.

DOI: 10.1103/PhysRevB.99.235435

I. INTRODUCTION

Graphene offers a promising platform to realize and explore the hydrodynamics of electrons [1]. Graphene serves as an excellent model system for theorists due to its simple electronic band structure; likewise, it is utilized by experimentalists for the relative ease of manufacturing pure samples. In certain thermodynamic regimes, the electrons in graphene become strongly interacting; hydrodynamics is a useful tool to study strongly interacting systems not amenable to ordinary perturbation methods. Hydrodynamics is applicable when systems rapidly thermalize and when both the mean-free path (l_{ee}) and mean-free time (τ_{ee}) are short compared to the relevant length and time scales of the problem [2]. When a system is in this regime, the main observables are conserved quantities: these are precisely the objects tracked by hydrodynamics.

Graphene has two different hydrodynamic regimes. When the chemical potential μ is much larger than the temperature, $k_B T \ll \mu$, graphene behaves like an ordinary conductor and is described by Fermi liquid theory. First discovered by Landau [3] in 1959, Fermi liquid theory treats the electrons as a noninteracting Fermi gas and then turns on interactions adiabatically; thus, Fermi liquids exhibit *weakly* interacting quasiparticles. The excitations, no longer pure electron states, are instead described as quasiparticles. Though weak interactions imply long mean-free paths, graphene can actually exhibit hydrodynamic effects in this regime. The electrons in graphene only weakly interact with phonons (which typically disrupt the hydrodynamic signature), so it is still possible to have $l_{ee} \ll l_{phonon}$. Likewise, graphene samples can be made very pure; therefore, the impurity scattering distances can be made large compared to the mean-free path as well ($l_{ee} \ll l_{imp}$).

In the opposite limit—i.e., when $\mu \ll k_B T$—graphene enters a strongly coupled state known as a Dirac fluid (also known as a "quantum critical regime"). In the Fermi liquid regime, the presence of a Fermi surface imposes strong kinematic constraints on the possible scattering pathways; this prevents electrons far from the Fermi surface from interacting strongly. However, near charge neutrality, the Fermi surface shrinks, allowing electrons to interact *strongly*. The bare coupling constant α_0 gives a measure of this interaction strength. In the Dirac regime of graphene, α_0 can be of order unity; renormalization reveals the coupling to be marginally irrelevant, but for many laboratory conditions, it can still be on the order of 0.1–0.5: see Lucas and Fong [1] for more details. This strong coupling makes Dirac fluids ideal candidates for hydrodynamic analysis.

A hydrodynamic analysis of electron motion in graphene is governed by a number of phenomenological parameters. A derivative expansion can be utilized to derive the hydrodynamics equations [1]. The first-order corrections contain three such parameters: the shear viscosity η, the bulk viscosity ζ, and the "intrinsic" conductivity σ_Q. These cannot be predicted from the hydrodynamic theory and must be measured or calculated microscopically.

A number of experiments have measured the value of intrinsic conductivity [4,5]. Similarly, there have been a number of experimental proposals [6–9] for measuring η. While there have been a few measurements [10,11] of η in the Dirac regime, many of the proposals—such as negative nonlocal resistance measurements [8]—only apply to the Fermi regime [1]. Therefore, different hydrodynamic predictions would be useful for investigating η in Dirac fluids.

Solitons—disturbances that propagate without changing shape, even after interacting with each other—serve as prototypical hydrodynamics phenomena amenable to analytic tools. Solitons are made possible when dispersion balances focusing-nonlinearities. Graphene's hydrodynamic regime supports collective electron/hole sound waves called "first-sound" modes [12] or "demons" [13]; these sound modes can become solitons if dispersion balances focusing. Akbari-Moghanjoughi [14] analyzed solitons and periodic waves in both the two- and three-dimensional (2D and 3D) completely degenerate ($T = 0$) Fermi regimes. Solitons are permitted due to the inherently nonlinear nature of the hydrodynamic equations; to capture this behavior, a Bernoulli pseudopotential was used to analyze the fully nonlinear equations. However, while this method predicted some parameters—such as minimum propagation speeds—it did not generate an analytic expression for the soliton's profile.

A different approach to studying solitons was presented by Svintsov *et al.* [15] using standard perturbation theory. This produced a Korteweg–de Vries (KdV) equation

to describe the solitons' propagation and generated analytic approximations to the disturbances' shapes. Unlike the analysis of Akbari-Moghanjoughi [14], this linearized approach lacked a dispersive term to balance the nonlinearities. Instead, the graphene was placed on a gated substrate; this provided a weak dispersive force that permitted the formation of solitons.

While the analysis of solitons by Svintsov *et al.* [15] provided a more concrete result, it was limited to inviscid Fermi liquids. The present study will extend the results to include the Dirac regime as well. Whereas Svintsov *et al.* [15] used kinetic theory, we will instead treat the system using a systematic hydrodynamic expansion. Additionally, this paper will extend the results of both Svintsov *et al.* [15] and Akbari-Moghanjoughi [14] by including the effects of dissipation. This allows us to propose new experiments to measure the viscosity of the electron fluid. The derivation presented here is applicable to either the Dirac ($\mu \ll k_B T$) or Fermi ($k_B T \ll \mu$) regime, though it is unable to interpolate between the two. Nevertheless, our proposal offers an advantage over transport measurements in that its interpretation is less theory-laden.

In Sec. II we will derive the governing equations. Section III will be devoted to the subtle aspects of normalization. Next, Sec. IV will detail the perturbation expansion for the special case of stationary solitons. Section V extends the analysis to the more general case of solitons on an arbitrary background flow. We will provide a short analysis of the results in Sec. VI. Finally, in Sec. VII, we will detail potential experimental setups using these solitons to measure graphene's viscosity.

II. GOVERNING EQUATIONS

The electrons in graphene satisfy a pseudorelativistic dispersion relation [1]

$$\varepsilon(\mathbf{p}) = \pm v_F |\mathbf{p}|, \tag{1}$$

with $\mathbf{p}$ the momentum, $v_F \approx c/300$ the Fermi velocity, and $\varepsilon(\mathbf{p})$ the energy density. This equation is valid near a Dirac point at $\mathbf{p} = 0$, and deviates from linearity when $|\mathbf{p}|a/\hbar \approx 1/2$ with a the distance between adjacent carbon atoms in the graphene.

Given the pseudorelativistic dispersion, it is natural to write the conserved currents in relativistic notation with $x^\mu = (v_F t, \mathbf{x})^\mu$ and $\partial_\mu = (\partial_t/v_F, \nabla)_\mu$. Ignoring impurity and phonon scattering, the equations of motion are [1]

$$\partial_\mu J^\mu = 0, \tag{2}$$

$$\partial_\mu T^{\mu\nu} = \frac{1}{v_F} F^{\nu\mu} J_\mu. \tag{3}$$

Here, $T^{\mu\nu}$ is the energy-momentum tensor, and $F^{\mu\nu}$ is the electromagnetic tensor (including self-interactions). Additionally, J^μ is the charge 4-current [16]. Note that we will be using Gaussian units with $e = |e|$ positive. Finally, we will include a factor of v_F in the timelike components of 4-vectors, like $x^\mu = (v_F t, \mathbf{x})^\mu$, so that the metric $g^{\mu\nu} = \mathrm{diag}(-1, 1, 1, 1)^{\mu\nu}$ is dimensionless.

It is often preferable to write these equations in terms of more conventional quantities such as the fluid 3-velocity $\mathbf{u}$ and the (rest-frame) number density of charge carriers, $n = (n_{\mathrm{el}} - n_{\mathrm{hol}})$, with n_{el} (n_{hol}) the number density of electrons (holes). To do so, J^μ and $T^{\mu\nu}$ are expanded in the small parameter $l_{\mathrm{ee}}\delta$. In this equation, l_{ee} is the electron-electron scattering mean free path and δ is a characteristic inverse length scale of the observables. Since $\delta \sim \partial$ (with the partial derivative acting on slow observables), this is called the derivative expansion: see Lucas and Fong [1] for more details.

The expansions for $T^{\mu\nu}$ and J^μ become unwieldy at higher orders, but truncating at order $l_{\mathrm{ee}}\delta$ [17] we find [1]

$$J^\mu = -enu^\mu + \frac{\sigma_Q}{e}\mathcal{P}^{\mu\nu}\left(\partial_\nu \mu - \frac{\mu}{T}\partial_\nu T + eF_{\nu\rho}u^\rho\right), \tag{4}$$

$$T^{\mu\nu} = (\varepsilon + P)\frac{u^\mu}{v_F}\frac{u^\nu}{v_F} + Pg^{\mu\nu} - \eta\mathcal{P}^{\mu\rho}\mathcal{P}^{\nu\alpha}\left(\partial_\rho u_\alpha + \partial_\alpha u_\rho - \frac{2}{d}g_{\rho\alpha}\partial_\beta u^\beta\right) - \zeta\mathcal{P}^{\mu\nu}\partial_\alpha u^\alpha, \tag{5}$$

with ε the energy density, P the pressure, μ the chemical potential, and T the temperature in the rest frame.

We have defined the spacelike projection operator $\mathcal{P}^{\mu\nu} := g^{\mu\nu} + u^\mu u^\nu/v_F^2$ and used $u^\mu u_\mu = -v_F^2$ to write the 4-velocity as $u^\mu = \gamma(v_F, \mathbf{u})$ with $\gamma = 1/\sqrt{1 - (|\mathbf{u}|/v_F)^2}$ a Lorentz factor. Further, we have chosen the Landau frame, where

$$u_\mu J^\mu = env_F^2 \quad \text{and} \quad u_\mu T^{\mu\nu} = -\varepsilon u^\mu. \tag{6}$$

It is sometimes more instructive to write out 4-vectors in terms of their 3-vector and timelike components. For instance, J^μ is

$$J^0 = -\gamma env_F + \frac{\sigma_Q}{e}\left[\frac{T\gamma^2}{v_F}\left(\frac{|\mathbf{u}|^2}{v_F^2}\frac{\partial}{\partial t} + \mathbf{u}\cdot\nabla\right)\left(\frac{\mu}{T}\right) + \gamma e\frac{\mathbf{E}\cdot\mathbf{u}}{v_F}\right], \tag{7}$$

$$\mathbf{J} = -\gamma en\mathbf{u} + \frac{\sigma_Q}{e}\left[T\left(\nabla + \gamma^2\frac{\mathbf{u}}{v_F^2}D\right)\left(\frac{\mu}{T}\right) + \gamma e\left(\mathbf{E} + \frac{\mathbf{u}}{v_F}\times\mathbf{B}\right)\right], \tag{8}$$

where $D := \partial_t + \mathbf{u}\cdot\nabla$ is a material derivative.

To facilitate comparison with the existing literature, it is useful to rewrite the spacelike components as $v_F\partial_\nu T^{i\nu} - u^i\partial_\nu T^{0\nu} = v_F F^{\mu i}J_\mu - u^i F^{\mu 0}J_\mu$. Thus, our system becomes

$$\partial_\mu J^\mu = 0, \tag{9}$$

$$\partial_\nu T^{0\nu} = F^{\mu 0}J_\mu, \tag{10}$$

$$v_F\partial_\nu T^{i\nu} - u^i\partial_\nu T^{0\nu} = v_F F^{\mu i}J_\mu - u^i F^{\mu 0}J_\mu. \tag{11}$$

A. Ideal fluid

It is illuminating to temporarily consider the dissipationless case $\sigma_Q = \eta = \zeta = 0$. We are then able to write Eqs. (9)–(11) in 3-vector notation as

$$\frac{\partial}{\partial t}(\gamma n) + \nabla\cdot(\gamma n\mathbf{u}) = 0, \tag{12}$$

$$\frac{\partial}{\partial t}[\gamma^2(\varepsilon + P)] + \nabla\cdot[\gamma^2(\varepsilon + P)\mathbf{u}] - \frac{\partial P}{\partial t} = -\gamma ne\mathbf{E}\cdot\mathbf{u}, \tag{13}$$

$$\gamma^2\frac{(\varepsilon+P)}{v_F^2}\left(\frac{\partial\mathbf{u}}{\partial t}+\mathbf{u}\cdot\nabla\mathbf{u}\right)+\left(\frac{\mathbf{u}}{v_F^2}\frac{\partial P}{\partial t}+\nabla P\right)$$
$$=-ne\gamma\left(\mathbf{E}+\frac{\mathbf{u}}{v_F}\times\mathbf{B}-\frac{\mathbf{u}}{v_F}\mathbf{E}\cdot\frac{\mathbf{u}}{v_F}\right). \quad (14)$$

Then, it is clear that Eqs. (9)–(11) represent charge, energy, and 3-momentum conservation, respectively.

B. Phonons and heat flow

We have neglected the interactions (emission, absorption, and scattering) with phonons in our governing equations, Eqs. (9)–(11); we will now attempt to justify that choice. First, we consider the momentum equation (11).

The hydrodynamic regime is relevant when the electron-electron interaction time t_{ee} is the smallest timescale: $t_{ee} \ll t_{char} \ll t_d$ with t_{char} the soliton's propagation timescale and t_d its dissipation timescale. Following the standard prescription [1,5,18,19], we will neglect phonon-induced momentum relaxation in the momentum conservation equation, Eq. (11), if the phonon-induced momentum-relaxation time $t_{\text{e-ph}}^{(p)}$ is much longer than the other timescales of interest, $t_{ee} \ll t_d \ll t_d \ll t_{\text{e-ph}}^{(p)}$.

To support the claim that such a regime exists, we now present sample numerical values that satisfy such a timescale hierarchy. Nevertheless, we stress that this is simply an example; the derivation in the remainder of the paper will be valid over a wide range of experimental parameters; see Appendix B for further details.

The electron-electron scattering time in the Dirac regime is [1]

$$t_{ee} \sim 0.1\,\text{ps}\left(\frac{100\,\text{K}}{T}\right). \quad (15)$$

At $T = 60\,\text{K}$, this gives $t_{ee} = 0.17\,\text{ps}$. Using the sample values chosen in Sec. VII, we find (cf., Sec. VII B) a characteristic propagation time of $t_{char} = 6.5\,\text{ps}$. In that same section, we calculate a decay time of $t_d \approx 44\,\text{ps}$. Finally, the electron-phonon momentum-relaxation time for acoustic phonons (with speed $v_s = 2\times10^4\,\text{ms}^{-1}$) is given by [20]

$$t_{\text{e-ph}}^{(p)} \sim \frac{10\,\text{ps}}{T/100\,\text{K}\sqrt{n/(10^{12}\,\text{cm}^{-2})}}. \quad (16)$$

This yields $t_{\text{e-ph}}^{(p)} = 280\,\text{ps}$. Therefore, we see that we have $t_{ee} \ll t_{char} \ll t_d \ll t_{\text{e-ph}}$. Thus, with the experimental values chosen here, phonon-induced momentum relaxation can be neglected from Eq. (11).

Importantly, as shown in recent experiments [5], there does appear to exist an experimentally realizable regime where the requisite hydrodynamic condition $t_{ee} \ll t_{char} \ll t_{\text{e-ph}}^{(p)}$ holds. Indeed, these experiments motivate us to suggest that such an approximation might be valid. Nevertheless, it would be useful to have a more refined estimate of the rate at which momentum and energy are lost to phonons.

1. Isothermal versus adiabatic

Now we consider the effect of phonons on the energy conservation equation (10). The energy conservation equation implicitly assumes our system is adiabatic: that is, the absence of energy sources/sinks presumes that heat neither enters nor leaves the system. In general, we could include terms (such as coupling to phonons) representing heat gain/loss. Instead, we could consider the opposite limit involving rapid heat transfer with the environment resulting in isothermal conditions. Under this assumption, the energy conservation equation is no longer needed; rather, the thermodynamic relations of Sec. II C could be used to relate our dynamic variables P and n, since T would no longer be dynamical. Therefore (as in the case of Newton's calculation of sound-speed in air), it is important to determine whether adiabatic or isothermal conditions are more applicable.

The most likely thermalization pathway would involve energy loss to phonons: the soliton's location in the middle of the sample minimizes heat advection through the edge contacts; similarly, radiative cooling is far too slow to thermalize the system on relevant timescales [21]. Indeed, if the graphene is placed on a substrate, phonons are responsible for the majority of the heat transfer to the environment [22,23].

For the isothermal condition to be applicable, the electrons must quickly lose energy to the environment: that is, the energy-relaxation time $t_{\text{e-ph}}^{(\varepsilon)}$ must satisfy $t_{\text{e-ph}}^{(\varepsilon)} \leqslant t_{ee} \ll t_{char} \ll t_{\text{e-ph}}^{(p)}$. However, single-phonon interactions are unlikely to extract heat quickly enough. Each phonon with wave number k carries a momentum $\hbar k$ while the electron fluid has momentum density $u(\varepsilon+P)/v_F^2 \sim u\varepsilon/v_F^2$. Likewise, phonons have energy $\hbar k v_s$ with sound-speed v_s, while the electrons have energy density ε. Recall that we require the electron-electron momentum exchange rate $\dot{p}_{ee}$ to be much greater than the electron-phonon momentum relaxation rate $\dot{p}_{\text{e-ph}}$ in order for hydrodynamics to be valid: $\dot{p}_{ee} \gg \dot{p}_{\text{e-ph}}$. However, multiplying by v_s and rewriting in terms of the energy exchange rates yields $\dot{\varepsilon}_{ee} u v_s/v_F^2 \gg \dot{\varepsilon}_{\text{e-ph}}$. Given that $v_s \approx 2\times10^4\,\text{m s}^{-1} \ll v_F$ for acoustic phonons [24] and $u \approx 4.0\times10^5\,\text{m s}^{-1} \sim v_F$ for our system, we see that $\dot{\varepsilon}_{ee} \gg \dot{\varepsilon}_{\text{e-ph}}$. Hence, if phonon-induced momentum relaxation can be neglected, so can phonon-induced energy relaxation.

For isothermal conditions to be applicable, other thermalization pathways must be available. For instance, multiphonon supercollisions [24] can increase the energy flux relative to the momentum flux. However, under the assumption of weak phonon coupling, we can ignore the influence of multiphonon processes. Therefore, in the absence of other energy-relaxation mechanisms, it appears that adiabatic conditions are more appropriate for our system, with $t_{ee} \ll t_{char} \ll t_{\text{e-ph}}^{(p)} \ll t_{\text{e-ph}}^{(\varepsilon)}$.

In the body of this paper, we will use isothermal conditions: these are more common in the literature [14,15] and are somewhat simpler. Nevertheless, adiabatic conditions appear to be more practical and are used for the derivation in Appendix C.

C. Thermodynamics

Currently, our system, Eqs. (9) and (11), is underdetermined. This can be remedied by including a thermodynamic equation of state to relate ε and P.

In graphene, the photonlike dispersion relation for the electrons gives the pressure as $P = \varepsilon d$, with d the dimension of the system ($d = 2$ for graphene) [1]. Graphene has a natural energy scale at which the band structure's curvature becomes

relevant. However, for temperatures much lower than this scale, $\Lambda \sim 10^4\,\mathrm{K}$, there are only two energy scales in the problem: $k_B T$ and μ. Therefore, from dimensional analysis, the pressure must be expressed as [1]

$$P(\mu, T) = \frac{(k_B T)^{d+1}}{(\hbar v_F)^d} F\left(\frac{\mu}{k_B T}\right) \tag{17}$$

for a function F subject to constraints imposed by the positivity of the entropy density $s = \partial P/\partial T \geqslant 0$. Additionally, since our system is charge conjugation symmetric with $\mu \to -\mu$, F must be an even function.

In the Dirac regime ($\mu \ll k_B T$), P can be expanded as

$$P(\mu, T) = \frac{(k_B T)^{d+1}}{(\hbar v_F)^d}\left[\mathcal{C}_0^D + \mathcal{C}_1^D\left(\frac{\mu}{k_B T}\right)^2 + \mathcal{C}_2^D\left(\frac{\mu}{k_B T}\right)^4 + \cdots\right]. \tag{Dirac: 18}$$

Similarly, the carrier density can be expressed as

$$n(\mu, T) = \frac{\partial P}{\partial \mu} = \frac{(k_B T)^d}{(\hbar v_F)^d}\frac{\mu}{k_B T}\left[2\mathcal{C}_1^D + 4\mathcal{C}_2^d\left(\frac{\mu}{k_B T}\right)^2 + \cdots\right]. \tag{Dirac: 19}$$

Instead, in the Fermi regime ($\mu \gg k_B T$), we can write P as

$$P(\mu, T) = \frac{|\mu|^{d+1}}{(\hbar v_F)^d}\left[\mathcal{C}_0^F + \mathcal{C}_1^F\left(\frac{k_B T}{\mu}\right)^2 + \mathcal{C}_2^F\left(\frac{k_B T}{\mu}\right)^4 + \cdots\right]. \tag{Fermi: 20}$$

Likewise, the carrier density is given by

$$n(\mu, T) = (d+1)\frac{|\mu|^d \mathrm{sgn}\mu}{(\hbar v_F)^d}\left[\mathcal{C}_0^F + \frac{d-1}{d+1}\mathcal{C}_1^F\left(\frac{k_B T}{\mu}\right)^2 + \frac{d-3}{d-1}\mathcal{C}_2^F\left(\frac{k_B T}{\mu}\right)^4 + \cdots\right]. \tag{Fermi: 21}$$

Throughout the remainder of this paper, we will generically write $\mathcal{C}_0, \mathcal{C}_1$, etc.; the current regime of interest will determine whether to use $\mathcal{C}^D$ or $\mathcal{C}^F$. Explicit expressions for these coefficients are given in Appendix A. It is important to reiterate that, for our isothermal system, T is not a dynamical quantity dependent on space or time, but is merely a parameter.

D. Electrostatics

While our electron fluid moves in d-dimensions ($d = 2$ for graphene), we will assume the electromagnetic field propagates in $d+1$ dimensions (i.e., 3-space for graphene, as usual). We are only concerned with the electric potential ϕ since the magnetic terms are smaller by a factor of $v_F/c \approx 1/300$. The self-interaction of the charge distribution $n(x,t)$ generates an electric potential in the Lorenz gauge as

$$-\frac{1}{c^2}\frac{\partial^2\phi}{\partial t^2} + \nabla^2\phi = -4\pi J^0 = -4\pi[-en(x,t)\gamma]. \tag{22}$$

Note that we are using the $(d+1)$-dimensional Laplacian. Neglecting the $1/c^2$ time derivative gives Poisson's equation. For instance, with $d = 2$ this gives

$$\phi(\mathbf{x}, t) = -e\int \frac{n(y,t)\gamma}{|x-y|}d^3y. \tag{23}$$

Making the quasistatic approximation $\partial_t/\partial_x \ll c$—so we can neglect electrodynamic effects like $\partial_t \mathbf{A}$—we find

$$\mathbf{E} = e\int \frac{(\mathbf{x}-\mathbf{y})n(y,t)\gamma}{|x-y|^3}d^3y. \tag{24}$$

This equation is highly nonlocal in n, and using it in the energy-momentum tensor equation would produce a complicated integrodifferential equation. While we can deal with this (via a Fourier transform) for the linear approximation, going to higher orders would necessarily involve convolutions.

The main problem with this setup is that the Coulomb force is long-ranged; we can simplify this by using conducting gates. Since the electric-field lines must be normal to conductors, placing conductors directly above and below the graphene will force $\mathbf{E}$ to be nearly normal to the graphene [15,25]. Therefore, the x-component E_x will necessarily be small and can be handled perturbatively.

We impose gates a distance d_1 above and d_2 below the sample and fill the intervening space with a dielectric of relative permittivity κ. This gives a potential (in $d = 2$) of the form [15]

$$\phi = \frac{-\alpha\hbar v_F d_1 d_2}{e\kappa(d_1+d_2)}\left(1 + \frac{d_1 d_2}{3}\frac{\partial^2}{\partial x^2}\right)(\gamma n) + O(d_i\partial_x)^4. \tag{25}$$

Naturally, the electric field is given by the negative gradient of ϕ. Here, we have assumed that $d_i\partial_x \ll 1$. Furthermore, we have replaced $4\pi e^2/\hbar v_F$ with $\alpha(T)$, the renormalized coupling constant; this accounts for the effect of screening and is given by [1]

$$\alpha(T) = \frac{4}{(4/\alpha_0) + \ln(10^4\,\mathrm{K}/T)}, \tag{26}$$

with $\alpha_0 \approx 1$ depending on the graphene's substrate. For the Dirac regime at $T = 60\,\mathrm{K}$ considered throughout this paper, this gives $\alpha \approx 0.439$.

For convenience, we will define the collection of coefficients

$$A := \frac{\alpha\hbar v_F d_1 d_2}{\kappa(d_1+d_2)}, \tag{27}$$

so that the potential is given as

$$\phi = -\frac{A}{e}\left(1 + \frac{d_1 d_2}{3}\frac{\partial^2}{\partial x^2}\right)(\gamma n) + O d_i\partial_x^4. \tag{28}$$

While Eq. (27) only applies for $d = 2$, we will use ϕ given by Eq. (28) for arbitrary dimension, with an appropriately chosen A.

The first term on the right-hand side of Eq. (28) represents the electric potential from a uniform charge density. The second term is a weakly nonlocal correction that causes a weak dispersion.

III. DIMENSIONS, UNITS, AND REGIME OF INTEREST

It will be helpful in the following sections to be rather precise in specifying a nondimensionalization scheme. For convenience, we will choose units where $k_B = \hbar = v_F = e = 1$. We still have one dimension unspecified; in order to fully specify our unit system, we will choose an arbitrary reference length $l_{\text{ref}} = 50\,\text{nm}$; this is chosen so that T is nondimensionalized to roughly unity (see below) [26].

In later sections, we will be performing a perturbation expansion to solve the nonlinear system of equations. There, we will use expansions of the form $f = f_0 + \epsilon f_1 + f_2\epsilon^2 + \cdots$ with $\epsilon \ll 1$ a small parameter representing the size of perturbations.

Choosing the order of the problem's variables is very important. When collecting terms in perturbation theory, we assume that all variables and constants are order $O(1)$; the relative magnitude of terms is given solely by powers of ϵ. Let us emphasize that, unlike the choice of parameters to normalize above, this choice of nondimensionalization *is* physically relevant and determines our regime of interest.

Nondimensionalization sets the relative size of different terms and corresponds to a specification of our location in parameter space. Indeed, this choice dictates which terms and processes are relevant and which are negligible. Equivalently, this process can be viewed through the lens of dimensional analysis. Our system has 17 variables (5 dynamic: n, u, ε, P, and μ; 11 static: x, t, k_BT, d_i, κ, σ_Q/e^2, η, ζ, $\hbar$, v_F, and l_{ref}; and the previously defined perturbation scale ϵ). In total, there are 3 independent physical units (mass, length, and time). Therefore, the Buckingham Pi theorem implies there are 14 dimensionless parameters.

However, these 14 dimensionless parameters are not all independent. Our 3 thermodynamic equations ($\varepsilon = Pd$, as well as the definitions of P and n) reduce this number to 11. Furthermore, we have not yet specialized to solitons: in Appendix B, we will use dominant balance to impose 4 additional restrictions arising from our conservation equations, Eqs. (9)–(11). This leaves a total of 7 independent nondimensional parameters: ϵ, m, p, q, $O(\sigma_Q\hbar)$, $O(\eta l_{\text{ref}}^d/\hbar)$, and $O(\zeta l_{\text{ref}}^d/\hbar)$, as defined in Appendix B [27].

Naturally, investigations of the Fermi and Dirac regimes entail different nondimensionalizations. Additionally, even without a set regime, there are different nondimensionalization choices highlighting different areas of parameter space. Appendix B outlines a general nondimensionalization using dominant balance that encompasses various parameter spaces in both the Dirac and Fermi regimes. For concreteness, we will examine one particular nondimensionalization in the Dirac regime in this section. Nevertheless, the equations and solutions generated in the remainder of the paper are largely similar for both the Dirac and Fermi regimes; we will explicitly highlight the few terms that do differ between the two regimes. The nondimensionalization utilized in the Fermi regime is laid out in Appendix B 1.

A. Dirac nondimensionalization

We will denote nondimensional variables with a caret. Restricting to the Dirac regime and using a bit of foresight, we will choose to nondimensionalize the dynamical and thermodynamic variables as follows:

$$\begin{aligned} n &= \epsilon^{(d+2)/4}\hat{n}l_{\text{ref}}^{-d}, & u &= \hat{u}v_F, \\ \varepsilon &= \epsilon^{(d+1)/4}\hat{\varepsilon}\hbar v_F l_{\text{ref}}^{-d-1}, & P &= \epsilon^{(d+1)/4}\hat{P}\hbar v_F l_{\text{ref}}^{-d-1}, \\ \mu &= \epsilon^{3/4}\hat{\mu}\hbar v_F l_{\text{ref}}^{-1}, \quad \text{and} & T &= \epsilon^{1/4}\hat{T}\hbar v_F l_{\text{ref}}^{-1}k_B^{-1}. \end{aligned} \tag{29}$$

Here, we made use of the fact that we are in the Dirac regime ($\mu/T \ll 1$) and the thermodynamic equations of Sec. II C by ensuring

$$O\left(nl_{\text{ref}}^d\right) = O\left[\frac{\mu l_{\text{ref}}^{d+1}}{\hbar v_F}\left(\frac{Tl_{\text{ref}}}{\hbar v_F}\right)^{d-1}\right] \tag{30}$$

and

$$O\left(\frac{Pl_{\text{ref}}^{d+1}}{\hbar v_F}\right) = O\left(\frac{k_BTl_{\text{ref}}}{\hbar v_F}\right)^{d+1}. \tag{31}$$

Note that we took μ to be small but finite; as we will see later, taking μ to be identically zero causes disturbances to be "frozen" in place.

The gating distance will be normalized as $d_i = l_{\text{ref}}\hat{d}_i\epsilon^{-(d+3)/4}$. The electrostatic coefficient A [defined for $d = 2$ in Eq. (27)] is normalized as $A = \hat{A}\epsilon^{-(d+3)/4}\hbar l_{\text{ref}}^{d-1}v_F$.

The dissipative "intrinsic" conductivity $\sigma_Q\hbar/e^2$ represents another nondimensional parameter in our problem. In the hydrodynamic regime for $d = 2$, we have [28]

$$\frac{\sigma_Q}{e^2} \approx \frac{0.760}{2\pi\hbar\alpha(T)^2}, \tag{32}$$

with $\alpha(T)$ given by Eq. (26). We see that for $T \approx 60\,\text{K}$, we have $\sigma_Q = 0.20e^2/\hbar$. Therefore, $\sigma_Q\hbar/e^2$ is now a second small parameter (in addition to ϵ). To make progress with our perturbation expansion, we need to fix the magnitude of $\sigma_Q\hbar/e^2$ relative to ϵ. Since we will later choose $\epsilon \sim 0.1$, we see that $\hat{\sigma}_Q = 0.20 \approx \sqrt{0.1}$. Thus, we will nondimensionalize σ_Q as $\sigma_Q = \hat{\sigma}_Q\epsilon^{1/2}e^2l_{\text{ref}}^{2-d}/\hbar$.

According to Lucas and Fong [1], near the charge neutrality point with $d = 2$, the shear viscosity is given by

$$\eta \approx 0.45\frac{(k_BT)^2}{\hbar v_F^2\alpha(T)^2}. \tag{33}$$

For $T \approx 60\,\text{K}$, we have $\eta l_{\text{ref}}^2/\hbar = 1.1$. Therefore, we will choose $\eta = \epsilon^0\hat{\eta}\hbar l_{\text{ref}}^{-d}$. Though the bulk viscosity ζ is expected to be much smaller than η (due to approximate scale invariance), our setup is only sensitive to $\zeta + 2\eta(1 - 1/d)$; therefore, we will simply choose $\zeta = \epsilon^0\hat{\zeta}\hbar l_{\text{ref}}^{-d}$ as well. We can safely take $\hat{\zeta} \to 0$ without affecting the derivation.

In performing a derivative expansion, it is assumed that the relevant variables (n, ε, etc.) vary on length scales $\xi \gg l_{\text{ee}}$. If we normalize the length scales by ξ as $x = \hat{x}\xi$, then the derivatives are normalized according to Appendix B as

$$\frac{\partial}{\partial x} = \frac{1}{\xi}\frac{\partial}{\partial\hat{x}} = \frac{l_{\text{ref}}}{\xi}\frac{1}{l_{\text{ref}}}\frac{\partial}{\partial\hat{x}} = \epsilon^{(d+5)/4}\frac{1}{l_{\text{ref}}}\frac{\partial}{\partial\hat{x}}. \tag{34}$$

For the remainder of this paper, carets denoting normalized variables will be dropped for convenience.

Note that, in addition to our perturbation expansion in terms of ϵ, we have already made use of two other expansions: one for ϕ expanding in $(\partial_x d_i)^2$ and one for $P(\mu, T)$

expanding in $(\mu/T)^2$. Using these normalizations, we see that both $(\partial_x d_i)^2$ and $(\mu/T)^2$ are of order ϵ, so all perturbation expansions in the problem have the same accuracy.

IV. PERTURBATION EXPANSION

To analyze Eqs. (9)–(11), it will be useful to expand the dependent variables in a perturbation series:

$$\mathbf{u} = \mathbf{u}_0 + \epsilon \mathbf{u}_1 + \epsilon^2 \mathbf{u}_2 + \cdots, \tag{35}$$

$$P = P_0 + \epsilon P_1 + \epsilon^2 P_2 + \cdots, \tag{36}$$

$$n = n_0 + \epsilon n_1 + \epsilon^2 n_2 + \cdots. \tag{37}$$

A. Perturbative thermodynamics

We will be using the thermodynamic relationships of Sec. II C to write μ and T in terms of n and P; however, since T is nondynamical, it will only have a constant T_0 component, but not a $T_1(x,t)$ contribution. It is useful to define m as the order of $(\mu_0/T_0)^2$; that is, $\epsilon^m := O[\mu/(k_B T)]^2$. For the nondimensionalization specified in Sec. III, $m = 1$.

Expanding the thermodynamic variables and collecting powers of ϵ yields the following relations for the Dirac regime:

$$P_0 = T_0^{d+1}\mathcal{C}_0, \tag{Dirac: 38}$$

$$n_0 = 2T_0^{d-1}\mu_0\mathcal{C}_1, \tag{Dirac: 39}$$

$$P_1 = P_0\left[\frac{\mathcal{C}_1}{\mathcal{C}_0}\left(\frac{\mu_0}{T_0}\right)^2\delta_{m,1}\right], \tag{Dirac: 40}$$

$$n_1 = n_0\left[\frac{\mu_1}{\mu_0} + 2\frac{\mathcal{C}_2}{\mathcal{C}_1}\left(\frac{\mu_0}{T_0}\right)^2\delta_{m,1}\right], \tag{Dirac: 41}$$

$$P_2 = P_0\left[\frac{T_2}{T_0}(d+1)\frac{(d+1)d}{2} + 2\frac{\mathcal{C}_1}{\mathcal{C}_0}\frac{\mu_1}{\mu_0}\left(\frac{\mu_0}{T_0}\right)^2\delta_{m,1} + \frac{\mathcal{C}_2}{\mathcal{C}_0}\left(\frac{\mu_0}{T_0}\right)^4\delta_{m,1} + \frac{\mathcal{C}_1}{\mathcal{C}_0}\left(\frac{\mu_0}{T_0}\right)^2\delta_{m,2}\right], \tag{Dirac: 42}$$

$$n_2 = n_0\left[\frac{\mu_2}{\mu_0} + \frac{T_2}{T_0}(d-1) + 6\frac{\mathcal{C}_2}{\mathcal{C}_1}\frac{\mu_1}{\mu_0}\left(\frac{\mu_0}{T_0}\right)^2\delta_{m,1} + 3\frac{\mathcal{C}_3}{\mathcal{C}_1}\left(\frac{\mu_0}{T_0}\right)^4\delta_{m,1} + 2\frac{\mathcal{C}_2}{\mathcal{C}_1}\left(\frac{\mu_0}{T_0}\right)^2\delta_{m,2}\right], \tag{Dirac: 43}$$

with $\delta_{a,b}$ the Kronecker delta function.

Similarly, for the Fermi regime, we find

$$P_0 = |\mu_0|^{d+1}\mathcal{C}_0, \tag{Fermi: 44}$$

$$n_0 = |\mu_0|^d \operatorname{sgn}(\mu_0)\mathcal{C}_0(d+1), \tag{Fermi: 45}$$

$$P_1 = P_0\left[\frac{\mu_1}{\mu_0}(d+1) + \frac{\mathcal{C}_1}{\mathcal{C}_0}\left(\frac{T_0}{\mu_0}\right)^2\delta_{m,-1}\right], \tag{Fermi: 46}$$

$$n_1 = n_0\left[\frac{\mu_1}{\mu_0}d + \frac{\mathcal{C}_1}{\mathcal{C}_0}\frac{d-1}{d+1}\left(\frac{T_0}{\mu_0}\right)^2\delta_{m,-1}\right], \tag{Fermi: 47}$$

$$P_2 = P_0\left[\frac{\mu_2}{\mu_0}(d+1) + \frac{\mu_1^2}{\mu_0^2}\frac{(d+1)d}{2} + \frac{\mathcal{C}_1}{\mathcal{C}_0}(d-1)\frac{\mu_1}{\mu_0}\left(\frac{T_0}{\mu_0}\right)^2\delta_{m,-1} + \frac{\mathcal{C}_2}{\mathcal{C}_0}\left(\frac{T_0}{\mu_0}\right)^4\delta_{m,-1} + \frac{\mathcal{C}_1}{\mathcal{C}_0}\left(\frac{T_0}{\mu_0}\right)^2\delta_{m,-2}\right]. \tag{Fermi: 48}$$

For leading order,

$$n_2 = n_0\left[\frac{\mu_2}{\mu_0}d + \frac{\mu_1^2}{\mu_0^2}\frac{d(d-1)}{2} + \frac{\mathcal{C}_1}{\mathcal{C}_0}\frac{(d-1)(d-2)}{d+1}\frac{\mu_1}{\mu_0}\left(\frac{T_0}{\mu_0}\right)^2\delta_{m,-1} + \frac{\mathcal{C}_2}{\mathcal{C}_0}\frac{d-3}{d+1}\left(\frac{T_0}{\mu_0}\right)^4\delta_{m,-1} + \frac{\mathcal{C}_1}{\mathcal{C}_0}\frac{d-1}{d+1}\left(\frac{T_0}{\mu_0}\right)^2\delta_{m,-2}\right]. \tag{Fermi: 49}$$

Using these equations, we can now write μ and P in terms of n at each order. In particular, we find

$$\frac{P_1}{P_0} = \frac{n_1}{n_0}K_0 + \frac{\mathcal{C}_1}{\mathcal{C}_0}\left(\frac{\mu_0}{T_0}\right)^{2m}\left(\delta_{m,1} + \frac{1}{d}\delta_{m,-1}\right). \tag{50}$$

Here, we have defined K_0 as

$$K_0 = \begin{cases} 0, & m > 0 \text{ (Dirac regime)}, \\ (d+1)/d, & m < 0 \text{ (Fermi regime)}. \end{cases} \tag{51}$$

As a side note, it is straightforward to show with thermodynamic identities that K_0 is the leading-order term in the ratio of bulk modulus B to pressure P; that is, $K_0 = B_0/P_0$.

B. Conservation equations

First, let us investigate a scenario with a constant, uniform background flow $u_0 \neq 0$ chosen such that the perturbations are stationary in the laboratory frame. This will both simplify the mathematics and be experimentally interesting. To accomplish this, we will only permit variations on long timescales (this will be important when including dissipation). Mathematically, we accomplish this by normalizing the time variable as $t = \epsilon \hat{t}_1 \xi / v_F$ such that $\partial_{t_1} = \epsilon O(\partial_{\hat{x}})$.

Expanding the governing equation, we find the following:

Leading order:

$$\frac{\partial}{\partial x}(\gamma^2 n_0 u_1 + u_0 n_1) = 0, \tag{52a}$$

$$\frac{\partial}{\partial x}\left[\gamma P_1 + u_0\gamma^3(\varepsilon_0 + P_0)u_1 + \gamma A n_0 n_1 + \gamma^3 A n_0^2 u_0 u_1\right] = 0. \tag{52b}$$

First-order correction:

$$\begin{aligned}
&\frac{\partial}{\partial x}(\gamma^2 n_0 u_2 + u_0 n_2) \\
&= -\gamma^2\big[u_0\gamma^2\big(2+u_0^2\big)n_0 u_1 + n_1 + n_0 u_0 u_1\big]\frac{\partial u_1}{\partial x} - \gamma^2 u_1\frac{\partial n_1}{\partial x} + \gamma u_0 A\sigma_Q\frac{\partial^2 n_1}{\partial t_0\partial x} + \gamma A\sigma_Q\frac{\partial^2 n_1}{\partial x^2} \\
&\quad + \gamma^3 u_0 A\sigma_Q n_0\left(\frac{\partial^2 u_1}{\partial x^2} + u_0\frac{\partial^2 u_1}{\partial t_0\partial x}\right) + \Theta(-m)\gamma\sigma_Q\frac{\partial^2}{\partial x^2}\left(\mu_1 - \frac{T_0}{\mu_0}T_1\right), \qquad (53a)\\
&\frac{\partial}{\partial x}\big[\gamma P_2 + u_0\gamma^3(\varepsilon_0+P_0)u_2 + \gamma A n_0 n_2 + \gamma^3 A n_0^2 u_0 u_2\big] \\
&= -\gamma^3\big[u_0(\varepsilon_1+P_1) + \big(1+u_0^2\big)u_1\gamma^2(\varepsilon_0+P_0)\big]\frac{\partial u_1}{\partial x} - A n_1\gamma\frac{\partial n_1}{\partial x} + A n_0 u_0 u_1\gamma^3\frac{\partial n_1}{\partial x} - \gamma A n_0\frac{d_1 d_2}{3}\frac{\partial^3 n_1}{\partial x^3} \\
&\quad - A n_0^2\big(1+u_0^2\big)u_1\gamma^5\frac{\partial u_1}{\partial x} - A n_0^2 u_0\gamma^3\frac{d_1 d_2}{3}\frac{\partial^3 u_1}{\partial x^3} - A n_0 u_0 u_1\gamma^3\frac{\partial n_1}{\partial x} - 2A n_0 u_0 n_1\gamma^3\frac{\partial u_1}{\partial x} \\
&\quad + \gamma^4\left[\zeta + 2\eta\left(1-\frac{1}{d}\right)\right]\left(u_0^2\frac{\partial^2 u_1}{\partial t_0^2} + 2u_0\frac{\partial^2 u_1}{\partial t_0\partial x^2} + \frac{\partial^3 u_1}{\partial x^2}\right). \qquad (53b)
\end{aligned}$$

Here, we have defined $\gamma = 1/\sqrt{1-u_0^2}$ (with $v_F = 1$) and used the electrostatic coupling A according to Eq. (28). Additionally, we have used the Heaviside function

$$\Theta(-m) = \begin{cases} 0, & m > 0 \text{ (Dirac regime)}, \\ 1, & m < 0 \text{ (Fermi regime)}. \end{cases} \qquad (54)$$

C. Leading-order equations

Using the thermodynamic relation $\varepsilon = Pd$, the leading-order equations can be manipulated as

$$\gamma^2 d\left(A n_0 + \frac{P_0 K_0}{n_0}\right)[\text{Eq. (52a)}] - \gamma d u_0[\text{Eq. (52b)}]$$

yielding

$$0 = \gamma^2 d\big\{A n_0^2 + \gamma^2 P_0\big[K_0 - u_0^2(d+1)\big]\big\}u_1. \qquad (55)$$

We want nontrivial perturbations $u_1 \neq 0$, so we require the terms in square brackets to vanish. We see that this gives an equation for u_0 required to make the leading-order solutions time-independent:

$$u_0 = \pm\sqrt{\frac{[K_0/(d+1)] + \big[A n_0^2/P_0(d+1)\big]}{1 + \big[A n_0^2/P_0(d+1)\big]}}. \qquad (56)$$

It is easy to check that $u_0^2 < 1$ for $d \neq 1$; this is required, otherwise $\gamma = 1/\sqrt{1-u_0^2}$ would be imaginary.

Additionally, if we restrict to solutions bounded in x, we can require each term inside ∂_x from Eqs. (52a) and (52b) to be zero, giving

$$u_1 = -\frac{u_0}{\gamma^2 n_0} n_1 + U_1. \qquad (57)$$

Here, we have included a constant, uniform current $U_1(x, t_0, t_1) = U_1$; this will allow us—at the next order—to cancel the disturbance's propagation speed (similar to our use of u_0 at this order).

D. First-order corrections

Now, we can do the same for the first-order corrections. Manipulating them as before,

$$\gamma^2 d\left(A n_0 + \frac{P_0 K_0}{n_0}\right)[\text{Eq. (53a)}] - \gamma d u_0[\text{Eq. (53b)}]$$

gives

$$\gamma^2 d\big\{A n_0^2 + \gamma^2 P_0\big[K_0 - u_0^2(d+1)\big]\big\}u_2 = \text{RHS}. \qquad (58)$$

Here, the right-hand side (RHS) depends only on n_1, u_1, ε_1, and P_1. However, inserting our solution for u_0 causes the left-hand side to vanish, giving us our desired compatibility condition on n_1. Thus, we have the compatibility equation

$$\mathcal{A}\frac{\partial n_1}{\partial t_1} + \mathcal{F}\frac{\partial n_1}{\partial x} + \mathcal{B} n_1\frac{\partial n_1}{\partial x} + \mathcal{C}\frac{\partial^3 n_1}{\partial x^3} = \mathcal{G}\frac{\partial^2 n_1}{\partial x^2}, \qquad (59)$$

with

$$\begin{aligned}
\mathcal{A} &= 2\gamma^2\frac{P_0 d}{n_0}u_0^2(d+1-K_0), && (60a)\\
\mathcal{B} &= -\gamma^2\frac{P_0}{n_0^2 d}u_0\big\{d^2 u_0^2[4(d+1) - K_0(d+3)] \\
&\quad + (d+1)\Theta(-m) - K_0 d^2\big\} && (60b)\\
\mathcal{C} &= -A d\frac{d_1 d_2}{3}n_0 u_0, && (60c)\\
\mathcal{F} &= \gamma^2\frac{P_0 d}{n_0}u_0\Bigg\{2U_1\gamma^2(d+1-K_0)u_0 \\
&\quad + \frac{\mathcal{C}_1}{\mathcal{C}_0}\left(\frac{\mu_0}{T_0}\right)^{2m}\left[u_0^2(d+1)\left(\frac{1}{d}\delta_{m,-1} + \delta_{m,1}\right)\right. \\
&\quad \left. - \left(\frac{d-1}{d^2}\delta_{m,-1} + 2\delta_{m,1}\right)\right]\Bigg\}, && (60d)
\end{aligned}$$

$$\mathcal{G} = \frac{\gamma^3}{n_0}\Bigg(\sigma_Q\gamma^2\left(\frac{P_0}{n_0}\right)^2 u_0^2(d+1)(d+1-K_0) \times\Bigg[d u_0^2 + \underbrace{\Theta(-m) - K_0\frac{d}{d+1}}_{=0}\Bigg] + d u_0^2\Bigg[\zeta + 2\eta\left(1-\frac{1}{d}\right)\Bigg]\Bigg). \tag{60e}$$

This is known as the KdV-Burgers (KdVB) equation. Note the underbraced term in $\mathcal{G}$ vanishes in both the Dirac and Fermi regimes.

E. Ideal fluid

Before tackling the full KdVB equation, it is beneficial to consider the simpler inviscid problem with $\sigma_Q = \eta = \zeta = 0$. In this case, we find $\mathcal{G} = 0$ and the KdV-Burgers equation reduces to the KdV equation. The KdV equation has soliton solutions of the form

$$n_1(x,t_1) = c_1\,\mathrm{sgn}(\mathcal{BC})\,\mathrm{sech}^2\left\{\sqrt{\frac{c_1|\mathcal{B}|}{12|\mathcal{C}|}} \times\left[x - \left(\frac{c_1|\mathcal{B}|}{3|\mathcal{A}|}\mathrm{sgn}(\mathcal{AC}) + \frac{\mathcal{F}}{\mathcal{A}}\right)t_1\right]\right\} \tag{61}$$

for arbitrary, order-1 constant $c_1 > 0$.

Substituting the coefficients, we find

$$n = n_0 + \epsilon c_1\,\mathrm{sgn}(\mathcal{BC})\,\mathrm{sech}^2\left(\frac{x+vt}{W}\right), \tag{62}$$

with

$$v = -\epsilon\left(\frac{c_1|\mathcal{B}|}{3|\mathcal{A}|}\mathrm{sgn}(\mathcal{AC}) + \frac{\mathcal{F}}{\mathcal{A}}\right) \tag{63}$$

and

$$W = \sqrt{\frac{12|\mathcal{C}|}{c_1|\mathcal{B}|}}. \tag{64}$$

Let us seek a soliton that is stationary in the laboratory frame; we have already accomplished $\partial_{t_0} n_1 = 0$ by a choice of u_0; we can similarly set $\partial_{t_1} n_1 = 0$ by an appropriate choice of U_1. If we choose U_1 so that $\mathcal{F} = -c_1\mathcal{B}/3\,\mathrm{sgn}\,\mathcal{BC}$, then the soliton is stationary:

$$n = n_0 + \epsilon c_1\,\mathrm{sgn}(\mathcal{BC})\,\mathrm{sech}^2\left(\frac{x}{W}\right). \tag{65}$$

F. Dissipation

Now, we return to the full KdVB equation (59). It does not appear that the KdV-Burgers equation with $\mathcal{G} \neq 0$ has an analytic, solitonic solution. However, if $\mathcal{G} \ll (\mathcal{A},\mathcal{B},\mathcal{C})$, then an approximate solution is given by Eq. (62) but with time-dependent c_1, as described in Mei *et al.* [29]. For clarity, we can factor out this smallness as $\mathcal{G} = \delta\tilde{\mathcal{G}}$ so that $\delta \ll 1$ and $\tilde{\mathcal{G}}$ is the same order as $\mathcal{A}$. Then, another short multiple scales expansion for n_1 can be done in $\delta = O(\mathcal{G}/\mathcal{A})$. To be consistent with our original perturbation series, we require that $\epsilon \ll \delta \ll 1$.

As usual, we expand n_1 as $n_1 = n_1^{(0)} + \delta n_1^{(1)}$ and $\partial_{t_1} = \partial_{\tau_0} + \delta\partial_{\tau_1}$. Then, to leading order, the equation

$$\mathcal{L}_0 n_1^{(0)} := \mathcal{A}\partial_{\tau_0} n_1^{(0)} + \mathcal{F}\partial_x n_1^{(0)} + \frac{\mathcal{B}}{2}\partial_x\left(n_1^{(0)}\right)^2 \tag{66}$$

$$+\mathcal{C}\partial_x^3 n_1^{(0)} = 0, \tag{67}$$

where we have again defined the linear operator $\mathcal{L}_1$ acting on $n_1^{(1)}$. This is the ordinary KdV equation; therefore, $n_1^{(0)}$ has the solution given by Eq. (61) with order-1 free parameter $c_1 > 0$.

At next order in δ, we must allow the constant c_1 to become time-dependent on a slow timescale $c_1 = c_1(\tau_1)$. Then, our equation is

$$\mathcal{L}_1 n_1^{(1)} := \mathcal{A}\partial_{\tau_0} n_1^{(1)} + \mathcal{F}\partial_x n_1^{(1)} + \mathcal{B}\partial_x\left(n_1^{(0)} n_1^{(1)}\right) + \mathcal{C}\partial_x^3 n_1^{(1)} = -\mathcal{A}\partial_{\tau_1} n_1^{(0)} + \tilde{\mathcal{G}}\partial_x^2 n_1^{(0)}, \tag{68}$$

where we have again defined the linear operator $\mathcal{L}_1$ acting on $n_1^{(1)}$.

For certain inhomogeneous terms in Eq. (68), it is possible to generate secular (i.e., unbounded) growth; since this is clearly no longer a localized solution, we wish to avoid this. Here, we will utilize a multiple scales approach, though it will differ slightly from the method used in Sec. V since the homogeneous operator $\mathcal{L}_0$ is nonlinear. Following the example of Mei *et al.* [29], we note that $\mathcal{L}_0$ and $-\mathcal{L}_1$ are adjoint:

$$\int dx\left(n_1^{(1)}\mathcal{L}_0 n_1^{(0)} + n_1^{(0)}\mathcal{L}_1 n_1^{(1)}\right) = 0. \tag{69}$$

Then, substituting the right-hand sides of Eqs. (67) and (68), we get the compatibility condition

$$\int n_1^{(0)}\left(\mathcal{A}\partial_{\tau_1} n_1^{(0)} - \tilde{\mathcal{G}}\partial_x^2 n_1^{(0)}\right)dx = 0. \tag{70}$$

Inserting the soliton solution for $n_1^{(0)}$, we get an equation for $c_1(\tau_1)$:

$$\dot{c}_1 = -\frac{c_1^2|\mathcal{B}|\tilde{\mathcal{G}}}{|\mathcal{C}|\mathcal{A}}\frac{4}{45}. \tag{71}$$

Then, solving this equation and converting back to time t_1 gives

$$c_1(t_1) = \frac{c_1(0)}{1+\frac{t_1}{t_d}} \quad \text{with} \quad t_d = \frac{45\mathcal{A}|\mathcal{C}|}{4c_1(0)\mathcal{G}|\mathcal{B}|}, \tag{72}$$

with $c_1(0)$ the initial value of the parameter $c_1(t_1)$. Recall that this is derived under the assumption that $\epsilon \ll O(\mathcal{G}/\mathcal{A}) \ll 1$.

Additionally, we can solve the KdV-Burgers equation numerically for arbitrary $\mathcal{G}$; this shows similar behavior to the analytic approximation (cf., Figs. 1 and 2). That is, the soliton slowly decays as it progresses.

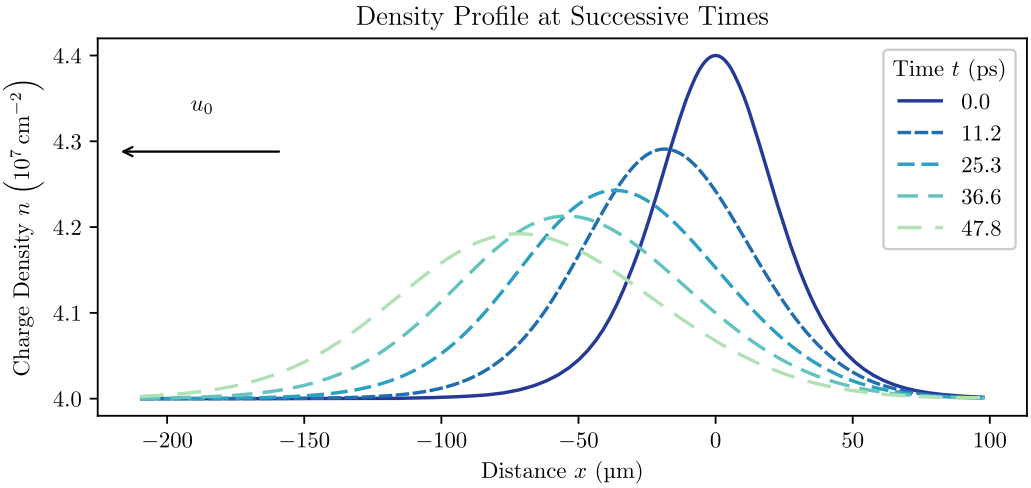

FIG. 1. Solitonic solution to KdV-Burgers. Values used were $\mathcal{A} = 0.88$, $\mathcal{B} = -0.70$, $\mathcal{C} = -0.060$, $\mathcal{F} = -1.1$, and $\mathcal{G} = 0.53$ with the height normalized to $4.0 \times 10^8\,\mathrm{cm}^{-2}$. This choice of parameters gives a soliton propagating in the $+x$ direction and a countercurrent u_0 in the $-x$ direction (indicated by the arrow).

V. MULTIPLE SCALES EXPANSION

Now, we wish to study the previous solitonic solution in more generality. Here, we will allow for an arbitrary uniform, time-independent background current u_0.

As we have seen previously, the nonlinearities affect the propagation velocity v [cf., Eq. (63)]. This is an example of a singular perturbation and requires the use of singular perturbation theory. Singular methods such as Poincaré-Lindstedt are only applicable to steady or periodic solutions. Since we are interested in decaying solutions, we need to make use of the method of multiple scales. Note that this approach is similar to that employed by Akbari-Moghanjoughi [30] in the study of partially degenerate electron-ion plasmas.

First, unlike the previous section, we will nondimensionalize the timescale so that $\partial_t = \partial_x$. Now, if we introduce a series of timescales $t_0 = t$, $t_1 = \epsilon t$, $t_2 = \epsilon^2 t, \ldots$ each presumed independent, the chain rule gives

$$\frac{\partial}{\partial t} = \frac{\partial}{\partial t_0} + \epsilon \frac{\partial}{\partial t_1} + \epsilon^2 \frac{\partial}{\partial t_2} + \ldots . \tag{73}$$

Further, we now assume that each variable is a function of all time scales: $n = n(x, t_0, t_1, t_2, \ldots)$.

If we again restrict to 1D motion and collect terms by powers of ϵ, we get the following equations:

Leading order:

$$\frac{\partial n_1}{\partial t_0} + \gamma^2 n_0 u_0 \frac{\partial u_1}{\partial t_0} + u_0 \frac{\partial n_1}{\partial x} + n_0 \gamma^2 \frac{\partial u_1}{\partial x} = 0, \tag{74a}$$

$$\gamma^3(\varepsilon_0 + P_0)\frac{\partial u_1}{\partial t_0} + \gamma u_0 \frac{\partial P_1}{\partial t_0} + u_0 \gamma^3(\varepsilon_0 + P_0)\frac{\partial u_1}{\partial x} + \gamma \frac{\partial P_1}{\partial x} + A n_0 \gamma \frac{\partial n_1}{\partial x} + A n_0^2 u_0 \gamma^3 \frac{\partial u_1}{\partial x} = 0. \tag{74b}$$

First-order correction:

$$\frac{\partial n_2}{\partial t_0} + \gamma^2 n_0 u_0 \frac{\partial u_2}{\partial t_0} + u_0 \frac{\partial n_2}{\partial x} + n_0 \gamma^2 \frac{\partial u_2}{\partial x} = \mathrm{RHS}, \tag{75a}$$

$$\gamma^3(\varepsilon_0 + P_0)\frac{\partial u_2}{\partial t_0} + \gamma u_0 \frac{\partial P_2}{\partial t_0} + u_0 \gamma^3(\varepsilon_0 + P_0)\frac{\partial u_2}{\partial x} + \gamma \frac{\partial P_2}{\partial x} + A n_0 \frac{\partial n_2}{\partial x} = \mathrm{RHS}. \tag{75b}$$

Again, we have used the electrostatic coupling A according to Eq. (28). See Appendix D for the terms on the right-hand side.

Notice that, as is often the case for multiple scales analyses, the linear operator acting on n_1, u_1, etc. in Eqs. (74a) and (74b) is identical to the linear operator acting on n_2, u_2, etc. in Eqs. (75a) and (75b). Furthermore, since this operator is linear, we do not need to employ the operator formalism of Sec. IV F, but can instead use a linear algebraic approach similar to Sec. IV (with the addition of another timescale, t_1).

A. Leading-order equations

Using $\varepsilon = Pd$ and combining equations like

$$\gamma^2 d\left[A n_0 \frac{\partial}{\partial x} + \frac{P_0 K_0}{n_0}\left(u_0 \frac{\partial}{\partial t_0} + \frac{\partial}{\partial x}\right)\right][\text{Eq. (74a)}]$$
$$-\gamma d\left(\frac{\partial}{\partial t_0} + u_0 \frac{\partial}{\partial x}\right)[\text{Eq. (74b)}]$$

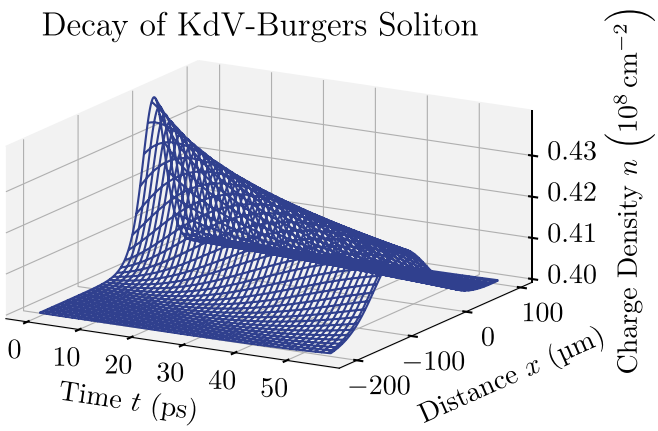

FIG. 2. Solitonic solution to KdV-Burgers showing decay as a function of time. Values used were $\mathcal{A} = 0.88$, $\mathcal{B} = -0.70$, $\mathcal{C} = 0.060$, $\mathcal{F} = -1.1$, and $\mathcal{G} = 0.53$ with the height normalized to $4.0 \times 10^8\,\mathrm{cm}^{-2}$.

gives

$$0 = \gamma^2 d\Big(-\gamma^2 P_0\big(d+1-u_0^2K_0\big)\frac{\partial^2 u_1}{\partial t_0^2} - 2\gamma^2 P_0 u_0(d+1-K_0)\frac{\partial^2 u_1}{\partial t_0 \partial x} + \big\{An_0^2 + \gamma^2 P_0\big[-u_0^2(d+1)+K_0\big]\big\}\frac{\partial^2 u_1}{\partial x^2}\Big). \tag{76}$$

This wave equation has solutions $f(x+v_0t_0)+g(x-v_0t_0)$ with v_0 given by

$$v_0^{(\pm)} = \frac{-u_0(d+1-K_0)}{d+1-u_0^2K_0} \pm \frac{1}{\gamma\big(d+1-u_0^2K_0\big)} \tag{77}$$

$$\times\sqrt{\frac{K_0(d+1)}{\gamma^2} + \frac{An_0^2}{P_0}\big(d+1-u_0^2K_0\big)}. \tag{78}$$

We will take the $(+)$ sign so that $v_0 = v_0^{(+)}$; the other can be recovered by taking $u_0 \to -u_0$ and $v_0 \to -v_0$. Further, we restrict to unidirectional solutions $u_1(x,t_0,t_1) = f(x \pm v_0t_0, t_1)$ for a definite choice of $\pm$; here, we choose $(+)$ as well—the other propagation direction can be recovered by taking $v_0 \to -v_0$.

For stationary perturbations ($v_0 = 0$), we can solve for u_0 to recover the result from Sec. IV:

$$u_0 = \pm\sqrt{\frac{[K_0/(d+1)] + \big[An_0^2/P_0(d+1)\big]}{1+\big[An_0^2/P_0(d+1)\big]}}. \tag{79}$$

For reference, the velocity of propagation in the absence of a background flow ($u_0 = 0$) is

$$v_0 = \pm\sqrt{\frac{1}{d+1}}\sqrt{K_0 + \frac{An_0^2}{P_0}}. \tag{80}$$

In general, n_1, u_1, and P_1 have traveling-wave solutions; neglecting solutions of the form $f(x-u_0t_0,t_1)$ that are simply advected by the background current, we find solutions given by

$$n_1(x,t_0,t_1) = n_1(x+v_0t_0,t_1) + F_1(t_1), \tag{81a}$$

$$u_1(x,t_0,t_1) = -\frac{(u_0+v_0)}{n_0\gamma^2(1+u_0v_0)}n_1(x+v_0t_0,t_1) + F_2(t_1). \tag{81b}$$

Here, we have arbitrary functions $F_1(t_1)$ and $F_2(t_2)$; by imposing boundary conditions $n_1 = 0$ at $x = \pm\infty$, we set $F_1 = 0$. We will allow $U_1(t_2) := F_2(t_2)$ to remain arbitrary; this uniform background current can be superimposed on the soliton solution as in Sec. IV if desired [31].

Now, we can also see why it was important to take $\mu_0 \ll T_0$ small but finite. Had $\mu = 0$ identically, then the thermodynamic relations would require $n_0 = 0$. Then, the leading-order charge conservation equation (74a) would give $\partial_{t_0}n_1 + u_0\partial_x n_1 = 0$; i.e., charge-density perturbations are simply advected along by the background flow. That is, the density perturbations lack any dynamic propagation and are "frozen-in." Since the other dependent variables are proportional to n_1, we see that P_1 and u_1 are similarly affected. Hence, if we want a dynamic disturbance, we require $\mu_0 \neq 0$; intuitively, this is understandable as there are no net charge carriers at the Dirac point.

B. First-order corrections

Now considering the first-order corrections, preventing secular growth of the higher-order terms (i.e., n_2, u_2, etc.) requires imposing a compatibility condition on the lower-order terms (i.e., n_1, u_1, etc.). We can manipulate the system as

$$\gamma^2 d\Big[An_0\frac{\partial}{\partial x} + \frac{P_0K_0}{n_0}\Big(u_0\frac{\partial}{\partial t_0} + \frac{\partial}{\partial x}\Big)\Big][\text{Eq. (75a)}] - \gamma d\Big(\frac{\partial}{\partial t_0} + u_0\frac{\partial}{\partial x}\Big)[\text{Eq. (75b)}],$$

which gives

$$\gamma^2 d\Big(-\gamma^2 P_0\big(d+1-u_0^2K_0\big)\frac{\partial^2 u_2}{\partial t_0^2} - 2\gamma^2 P_0 u_0(d+1-K_0)\frac{\partial^2 u_2}{\partial t_0\partial x} + \big\{An_0^2 + \gamma^2 P_0\big[-u_0^2(d+1)+K_0\big]\big\}\frac{\partial^2 u_2}{\partial x^2}\Big) = \text{LOT}, \tag{82}$$

where LOT represents lower-order terms (i.e., n_1, u_1, etc.).

It is instructive here to change variables to $\chi_0^{(\pm)} = x + v_0^{(\pm)}t_0$. Then, the equation becomes

$$\gamma^4 P_0 d\big(d+1-u_0^2K_0\big)(v_0^{(+)} - v_0^{(-)})^2\frac{\partial}{\partial\chi_0^{(-)}}\frac{\partial}{\partial\chi_0^{(+)}}u_2 = \text{LOT}. \tag{83}$$

This is where we encounter an apparent problem. Upon inserting our solutions for the lower-order terms, we find that the right-hand side depends on products and derivatives of $f(\chi_0^{(+)})$. This implies that the LOT are solely functions of $\chi_0^{(+)}$.

However, we see that functions of the form $f(\chi^{(+)})$ are also solutions to the homogeneous equation in Eq. (82) due to the presence of the $\partial_{\chi_0^{(-)}}$ operator.

So, products and derivatives of $f(\chi_0^{(+)})$ appear as inhomogeneous forcing terms that give rise to secular terms. For instance, terms proportional to $f^{(4)}(\chi_0^{(+)})$ give rise to solutions of the form $\chi_0^{(-)} f^{(3)}(\chi_0^{(+)})$. This grows unbounded in $\chi_0^{(-)}$—and hence, in time t. This will eventually cause $|u_2| > |u_1|$, invalidating the perturbation expansion. Thus, unless the LOT vanish identically, they will give rise to $\chi_0^{(\pm)}$-secular terms in u_2—i.e., solutions growing unbounded in t_0 or x.

Hence, we require the right-hand side to vanish and are left with the desired compatibility equation:

$$0 = \frac{\partial}{\partial \chi_0^{(+)}}(\mathrm{KdVB}[n_1]). \tag{84}$$

Here, $(\mathrm{KdVB}[n_1])$ represents the Korteweg–de Vries-Burgers equation, discussed earlier, acting on n_1:

$$\mathcal{A}'\frac{\partial n_1}{\partial t_1} + \mathcal{F}'\frac{\partial n_1}{\partial \chi_0^{(+)}} + \mathcal{B}' n_1 \frac{\partial n_1}{\partial \chi_0^{(+)}} + \mathcal{C}'\frac{\partial^3 n_1}{\partial \chi_0^{(+)^3}} - \mathcal{G}'\frac{\partial^2 n_1}{\chi_0^{(+)^2}} n_1 = 0; \tag{85}$$

see Appendix E for the functional form of the coefficients.

The solution to the KdV-Burgers equation was already derived in Sec. IV F and is simply reiterated here for convenience:

$$n_1(\chi_0^{(+)}, t_1) = c_1(t_1)\mathrm{sgn}(\mathcal{B}'\mathcal{C}')\mathrm{sech}^2\left\{\sqrt{\frac{c_1|\mathcal{B}'|}{12|\mathcal{C}'|}} \times \left[\chi_0^{(+)} - \left(\frac{c_1|\mathcal{B}'|}{3|\mathcal{A}'|}\mathrm{sgn}(\mathcal{A}'\mathcal{C}') + \frac{\mathcal{F}'}{\mathcal{A}'}\right)t_1\right]\right\}, \tag{86}$$

where

$$c_1(t_1) = \frac{c_1(0)}{1 + t_1/t_d} \tag{87}$$

with

$$t_d = \frac{45\mathcal{A}'|\mathcal{C}'|}{4c_1(0)|\mathcal{B}'|\mathcal{G}'}, \tag{88}$$

with $c_1(0)$ the initial amplitude of the soliton.

VI. ANALYSIS

Nondimensionalizing helped ensure that all quantities were order $O(1)$ and any information about their magnitude was solely contained in ϵ prefactors. However, having ordinary, dimensional expressions is more useful for comparing with experiments or existing literature. Therefore, the KdV-Burgers coefficients are written in terms of ordinary, dimensional variables in Appendixes E and F [32]. Note that the coefficients are still dimensionless and order unity [33].

The observables that characterize the system, to this order, are the amplitude, width, speed, and decay period of the soliton. The amplitude is simply given by

$$\|n_1\| = l_{\mathrm{ref}}^{-d}\epsilon^{(d+2)/4}\epsilon c_1(t)\mathrm{sgn}(\mathcal{B}'\mathcal{C}') := n_{\max}. \tag{89}$$

We can use $n_{\max}$ to eliminate c_1 in the following expressions [34]. Furthermore, we will factor out the explicit factors of ϵ and l_{ref} from the KdV-Burgers coefficients; we will denote the original, order unity, coefficients with a caret. Then, we can write the speed as

$$\begin{aligned} v &:= v_0 - \epsilon v_F\left(\frac{c_1\hat{\mathcal{B}}'}{3\hat{\mathcal{A}}'}\mathrm{sgn}(\mathcal{B}'\mathcal{C}') + \frac{\hat{\mathcal{F}}'}{\hat{\mathcal{A}}'}\right) \\ &= v_0 - \frac{n_{\max}\mathcal{B}'}{3\mathcal{A}'} - v_F\frac{\mathcal{F}'}{\mathcal{A}'}. \end{aligned} \tag{90}$$

Similarly, the width is given by

$$W := \xi\sqrt{\frac{12|\hat{\mathcal{C}}'|}{c_1|\hat{\mathcal{B}}'|}} = \sqrt{\frac{12\mathcal{C}'}{n_{\max}\mathcal{B}'}}. \tag{91}$$

Finally, the soliton decays with

$$n_{\max}(t) := l_{\mathrm{ref}}^{-d}\epsilon^{(d+6)/4}c_1(t)\mathrm{sgn}(\mathcal{B}'\mathcal{C}') = \frac{n_{\max}(0)}{1 + t/t_d}, \tag{92}$$

and the decay period is

$$t_d := \frac{1}{\epsilon}\frac{45\hat{\mathcal{A}}'|\hat{\mathcal{C}}'|\xi}{4c_1(0)\hat{\mathcal{G}}'|\hat{\mathcal{B}}|'v_F} = \frac{45\mathcal{A}'\mathcal{C}'}{4n_{\max}(0)v_F\mathcal{G}'\mathcal{B}'}. \tag{93}$$

Here, $n_{\max}(0)$ is the initial value of $n_{\max}$. The factor of ϵ in the first equality came from converting our $\hat{t}_1/\hat{t}_d$ to $t\epsilon\xi/\hat{t}_d v_F := t/t_d$.

We see that, upon redimensionalizing, c_1 and ϵ never appear alone. Therefore, simply defining $n_{\max}$ as their combination causes all ϵ and c_1 to drop out, showing that this is a one-parameter family of solutions. Note that these results hold in general for all nondimensionalizations specified in Appendix B. Similarly, notice that the factors of l_{ref} have all canceled: the observables are all independent of l_{ref}, as they must be since l_{ref} is arbitrary.

As mentioned in Sec. III, not all of the system's parameters are independent. It is helpful to reiterate here which can be set freely. Taking into account the thermodynamic relations, one experimentally useful set of independent parameters would be T_0, n_0, $n_{\max}(0)$, $u = u_0 + \epsilon U_1$, d_1, d_2, and κ.

A. Relation to previous results

As mentioned in the Introduction, Svintsov *et al.* [15] performed a similar perturbative analysis of solitons, though that analysis was restricted to the inviscid, Fermi liquid regime. It is straightforward to compare the inviscid results presented in Sec. IV E to those of Svintsov *et al.* [15].

First, our results for v_0 in the case of no background flow, $u_0 = 0$, are in agreement for the regime where $\mu/T \gg 1$ and $\mu/T > 0$, but they differ otherwise. However, this is to be expected: in setting up the problem, Svintsov *et al.* [15] neglect the contribution of holes. If the contribution of holes is included in their thermodynamic quantities, then our results are in agreement in both Fermi regimes, $|\mu/T| \gg 1$.

Nevertheless, the leading-order Dirac-regime speed v_0 used by Svintsov *et al.* [15] and derived in Svintsov *et al.* [35] has a minor error. There, the terms $ik^2\Sigma_j^2 v_F/\omega\langle p_j^{-1}\rangle$, with $j = e$ or h for electrons/holes, appear in Eqs. (28) and (29) of Ref. [35]. These terms arise from the

$\nabla(v_F\langle p_j\rangle)/2$ terms in the momentum conservation equations, Eqs. (8) and (9) of Ref. [35]. This corresponds to our pressure terms ∇P_j (though we combine P_e and P_h as $P = P_e + P_h$). The issue arises when Svintsov *et al.* [35] restrict to leading-order terms when calculating v_0. As we showed in Eq. (50), $\nabla P/P \sim \epsilon^2$ in the Dirac regime (i.e., $K_0 = 0$), while the inclusion of these $ik^2\Sigma_j^2 v_F/\omega\langle p_j^{-1}\rangle$ terms in Svintsov *et al.* [35] implicitly assumes $\nabla P/P \sim \epsilon$. On removing these terms from the leading-order equations, the results of Svintsov *et al.* [35] are consistent with ours.

Furthermore, the Fermi-Dirac distribution function chosen by Svintsov *et al.* [15] differs from the one chosen by Lucas and Fong [1] (and hence used in this paper): Svintsov *et al.* [15] chose $f(\mathbf{p})$ as

$$f(\mathbf{p}) = \frac{1}{1+\exp\{[\varepsilon(\mathbf{p}) - \mathbf{u}\cdot\mathbf{p} - \mu]/k_BT\}}, \tag{94}$$

while Lucas and Fong [1] chose the manifestly covariant

$$f(\mathbf{p}) = \frac{1}{1+\exp[(p^\nu u_\nu - \mu)/k_BT]}, \tag{95}$$

with $p^\nu = (|\mathbf{p}|, \mathbf{p})$ and $u^\nu = (1,\mathbf{u})/\sqrt{1-|\mathbf{u}|^2/v_F^2}$. This choice of distribution function is preferable as it preserves the form of the dispersion relation $\varepsilon = v_F|\mathbf{p}|$ under Lorentz boosts [with $\gamma = 1/\sqrt{1-(u/v_F)^2}$].

After accounting for these differences, our results are nearly in agreement. A few typographical errors [36] remain in the KdV equation and corresponding soliton solution and dispersion relation of Svintsov *et al.* [15]. After repairing these errors, we have consistent solutions and dispersion relations.

It is worth noting that Svintsov *et al.* [15] also use an isothermal assumption, though it is not directly stated; this assumption is utilized when stating the formula [37]

$$\frac{d\varepsilon}{\varepsilon} = 2\xi\frac{dn}{n} + (3-4\xi)\frac{dT}{T}, \tag{96}$$

with $\xi := n^2/\varepsilon\langle\varepsilon^{-1}\rangle$, and $\langle\varepsilon^{-1}\rangle \neq \varepsilon^{-1}$ is the average inverse energy. While ε depends on both n and T, the corresponding formula for $d\varepsilon/\varepsilon$ in Svintsov *et al.* [15] only has the dn/n term. In the Fermi regime, $|\mu/T| \gg 1$ and $\xi = 3/4$, so this is a valid simplification. However, in the Dirac regime, $\xi \ll 1$, and the dT/T term cannot be neglected unless the system is isothermal, $dT = 0$.

B. Role of gating

Our setup involves the use of conducting gates to screen the electrostatic interactions and make the problem local, and hence more mathematically tractable. However, Akbari-Moghanjoughi [14] instead considered solitons in ungated graphene; that analysis was restricted to the inviscid, $T = 0$ Fermi regime with no background flow [38]. While Akbari-Moghanjoughi [14] also derived solitonic solutions, a number of the properties differed markedly from those derived here.

First, Akbari-Moghanjoughi [14] found that there exists a critical propagation velocity v_c that separates periodic, wavelike solutions ($v < v_c$) and solitonic solutions ($v > v_c$). This was found to be $v_c = 3/\sqrt{38}$ for $d = 2$ and $v_c = 2/3$ for $d = 3$. However, there appears to be a small error in the derivation: Eq. (7) for ϕ involves a term $n^{-2/3}$ that should be $n^{-3/2}$. Repeating the derivation with this change shows that the critical propagation velocity is actually $v_c = 1/\sqrt{d}$. Our ($u_0 = 0$, Fermi regime) solutions have velocity

$$v = \frac{1}{\sqrt{d}}\sqrt{1+\frac{An_0^2 d}{P_0(d+1)}} + \epsilon v_1 \geqslant \frac{1}{\sqrt{d}} = v_c, \tag{97}$$

where we have used the fact that $\operatorname{sgn} v_1 = \operatorname{sgn} v_0$. Thus, we see that our soliton's speeds are bounded *below* by the critical speed, while Akbari-Moghanjoughi [14] found that soliton speeds should be bounded *above* by the critical speed.

Another difference involves the relation between the soliton height and speed. Using our expression for v_1, we found that the total speed with $u_0 = 0$ is

$$v = v_0\left(1+\epsilon\frac{c_1|\mathcal{B}|}{3|v_0\mathcal{A}|}\right) \tag{98}$$

while the soliton height is ϵc_1, with a free parameter $c_1 > 0$ [39]. Thus, increasing the height corresponds to increasing the speed, and vice versa. However, Akbari-Moghanjoughi [14] found that increasing the height causes the speed to *decrease*. Nevertheless, we both find the same, inverse relation between the height and width (as required by total charge conservation).

Furthermore, Akbari-Moghanjoughi [14] finds only dark ($n_1/n_0 < 0$) solitons. However, our solutions only give *bright* ($n_1/n_0 > 0$) solitons. Referring to Eq. (86), we have $\operatorname{sgn}(n_1) = \operatorname{sgn}(\mathcal{B}'\mathcal{C}')$. Here, we will consider the Dirac ($m > 0$) and Fermi ($m < 0$) cases separately. For the Dirac regime, with $K_0 = 0$, it is readily apparent that $\mathcal{B}'\mathcal{C}'$ (cf., Appendix E) is positive, yielding bright solitons.

Showing that the same holds true in the Fermi regime, with $K_0 = (d+1)/d$, is more involved. Using the expressions for $\mathcal{B}'$ and $\mathcal{C}'$ from Appendix E, we see

$$\operatorname{sgn}\left(\frac{n_1}{n_0}\right) = \operatorname{sgn}[3d(u_0+v_0)^2 - (1+u_0v_0)^2]. \tag{99}$$

We see that this is clearly positive when $u_0 = 0$; using the expression for v_0, we find it only crosses zero [40] when u_0 is given by

$$u_0 = \pm 1 \quad \text{or} \frac{\sqrt{2\lambda(3d-1)+4} \pm \lambda\sqrt{3d}}{2-\lambda} \quad \text{or} -\frac{\sqrt{2\lambda(3d-1)+4} \pm \lambda\sqrt{3d}}{2-\lambda}, \tag{100}$$

with $\lambda := An_0^2/P_0(d+1)$ as before. Finally, it can be checked that each of these solutions is larger (in magnitude) than unity; that is, $\mathcal{B}'\mathcal{C}'$ does not cross zero in the range $u_0 \in (-1,1)$. Thus, for $|u_0| < 1$, we find that $n_1/n_0 > 0$, and only bright solitons are permitted. Note that the adiabatic $\mathcal{B}'$ and $\mathcal{C}'$ coefficients in Appendix F are identical to their isothermal Fermi counterparts: therefore, the same reasoning shows the adiabatic system only has bright solutions, too.

Thus, it appears that a number of our findings are directly opposed to those of Akbari-Moghanjoughi [14]. While one might be tempted to compare the results of Akbari-Moghanjoughi [14] with our solutions by taking the gating distance $d_i \to \infty$, various quantities (e.g., v_0, W, etc.) would no longer be order-1, violating our expansion assumptions.

Instead, it appears that the presence or absence of gates can create qualitatively different results. However, this should not be surprising: the electric field with gates is given by derivatives of the density $E \propto \partial_x n + (d_1 d_2/3)\partial_x^3 n + \cdots$. On the other hand, the electric field without gates is given by the *antiderivative* of n: $E(x) \propto \int dy\, n(x)/|x-y|^2$. More specifically, the x-k Fourier transform of the electric potential with gates is $\hat{\phi} \propto (1 - k^2 d_1 d_2/3 + \cdots)\hat{n}$; highly dispersive, large k-modes *increase* the electric field's magnitude. The potential without gates is $\hat{\phi} \propto -\hat{n}/k^2$, so large k-modes *decrease* the electric field's magnitude. Given that this is the only difference between the setup of the two problems, it appears that this is the origin of the differences in the results [41].

C. Energy and entropy

It is interesting to determine the rate of energy loss by the soliton to dissipation. We can accomplish this by integrating the KdV-Burgers equation (59). Using Eq. (81b) to replace n_1 with u_1, we get (with new coefficients denoted by primes)

$$\mathcal{A}'\partial_{t_1} u_1 + \mathcal{F}'\partial_x u_1 + \mathcal{C}'\partial_x^3 u_1 + \mathcal{B}' u_1 \partial_x u_1 = \mathcal{G}'\partial_x^2 u_1. \tag{101}$$

Multiplying this equation by u_1 gives

$$\begin{aligned} &\tfrac{1}{2}\mathcal{A}'\partial_{t_1} u_1^2 + \tfrac{1}{2}\mathcal{F}'\partial_x u_1^2 + \mathcal{C}'\partial_x\big(u_1\partial_x^2 u_1\big) \\ &\quad -\tfrac{1}{2}\mathcal{C}'\partial_x(\partial_x u_1)^2 + \tfrac{1}{3}\mathcal{B}'\partial_x u_1^3 \\ &\quad = \mathcal{G}'\partial_x(u_1\partial_x u_1) - \mathcal{G}'(\partial_x u_1)^2. \end{aligned} \tag{102}$$

If we integrate once over all of x-space and impose boundary conditions $u_1 = \partial_x u_1 = 0$ at $x = \pm\infty$, we find

$$\frac{1}{2}\left(\partial_{t_1} + \frac{\mathcal{F}'}{\mathcal{A}'}\partial_x\right)\int dx\, u_1^2 = -\frac{\mathcal{G}'}{\mathcal{A}'}\int dx(\partial_x u_1)^2. \tag{103}$$

The left-hand side represents the time rate-of-change of the kinetic energy in a moving reference frame; this is more easily seen if the background current U_1 is removed so $\mathcal{F}' = 0$.

Using the expressions for $\mathcal{A}'$ and $\mathcal{G}'$ (cf., Appendix E), the right-hand side is negative semidefinite for the case with no background flow $u_0 = 0$. Thus, we see that—as expected—the viscosity causes the kinetic energy to decrease.

When $u_0 \neq 0$, it is more difficult to see that $\mathcal{G}'/\mathcal{A}' \geqslant 0$, as it must be for viscosity to remove energy. Here, we will again treat the Dirac and Fermi regimes separately. Starting with the Dirac case and using the expressions for $\mathcal{A}'$ and $\mathcal{G}'$ from Appendix E, we find

$$\begin{aligned} \operatorname{sgn}\left(\frac{\mathcal{G}'}{\mathcal{A}'}\right) = \operatorname{sgn}\Bigg\{&\sigma_Q\gamma^2\left(\frac{P_0}{n_0}\right)^2\frac{(u_0+v_0)^4}{1+u_0v_0}(d+1)^2 \\ &+ (u_0+v_0)^2\left[\zeta + 2\eta\left(1-\frac{1}{d}\right)\right]\Bigg\}. \end{aligned} \tag{104}$$

The only questionable term is $\sigma_Q/(1+u_0v_0)$. This term is positive for

$$|u_0| < \frac{1}{\sqrt{1+\big[An_0^2/P_0(d+1)\big]}}. \tag{105}$$

However, it blows up when $|u_0| \to 1/\sqrt{1+\lambda}$, with $\lambda := An_0^2/P_0(d+1)$. This causes u_1 and P_1 to become unbounded and invalidates our perturbation expansion. Thus, $|u_0| < 1/\sqrt{1+\lambda}$ is a constraint on the allowed parameters that make our derivation consistent. Under this constraint, $\mathcal{A}'\mathcal{G}' \geqslant 0$ in the Dirac regime, as it must be.

In the Fermi regime, we instead have

$$\begin{aligned} \operatorname{sgn}\left(\frac{\mathcal{G}'}{\mathcal{A}'}\right) = \operatorname{sgn}\Bigg(&\sigma_Q\gamma^2\left(\frac{P_0}{n_0}\right)^2(d+1)\frac{(u_0+v_0)^2}{(1+u_0v_0)} \\ &+\frac{d}{d+1}\frac{(u_0+v_0)^2\big[\zeta+2\eta\big(1-\frac{1}{d}\big)\big]}{(u_0+v_0)\big[v_0\big(d-u_0^2\big)+u_0(d-1)\big]}\Bigg). \end{aligned} \tag{106}$$

It is easy to show [42] that $(u_0+v_0)[v_0(d-u_0^2)+u_0(d-1)] > 0$ for $d > 1$ and $|u_0| < 1$; recall that we already required $|u_0| < 1$, otherwise $\gamma = 1/\sqrt{1-u_0^2}$ would blow up. Therefore, the η and ζ terms are positive.

As in the Dirac regime, we also have a $\sigma_Q/(1+u_0v_0)$ term. Though v_0 is different in the Fermi regime, the same reasoning also shows that this quantity is similarly positive for $|u_0| < 1/\sqrt{1+\lambda}$. Thus, as long as $|u_0| < 1/\sqrt{1+\lambda}$, we see that our theory is well-defined, $\mathcal{A}'\mathcal{G}' \geqslant 0$, and viscosity causes energy to decrease, as required by the second law of thermodynamics. Finally, note that the adiabatic $\mathcal{G}'$ in Appendix F differs slightly from this isothermal Fermi $\mathcal{G}'$; nevertheless, it shares the same questionable terms. Thus, the same exact reasoning shows $\mathcal{G}'/\mathcal{A}' \geqslant 0$ for the adiabatic regime [43].

To further investigate the soliton's decay, it is helpful to analyze entropy generation. Lucas and Fong [1] provide the following formula [44] for the divergence of the entropy current s^μ,

$$\begin{aligned} \partial_\mu s^\mu = \frac{1}{T}\partial_\mu u_\nu\Bigg[&\eta\mathcal{P}^{\mu\rho}\mathcal{P}^{\nu\alpha}\left(\partial_\rho u_\alpha + \partial_\alpha u_\rho - \frac{2}{d}g_{\rho\alpha}\partial_\beta u^\beta\right) \\ &+\zeta\mathcal{P}^{\mu\nu}\partial_\alpha u^\alpha\Bigg] + \frac{\sigma_Q}{T}\left(T\,\partial_\mu\frac{\mu}{T} + F_{\mu\rho}u^\rho\right) \\ &\times\mathcal{P}^{\mu\nu}\left(T\,\partial_\nu\frac{\mu}{T} + F_{\nu\rho}u^\rho\right). \end{aligned} \tag{107}$$

For simplicity, consider the case with no background flow, $u_0 = U_1 = 0$. Upon implementing our usual nondimensionalization in the Dirac regime (cf., Sec. III), we see the highest-order terms are

$$\partial_\mu s^\mu = \frac{\eta}{T_0}\partial^i u_1^j\left[\partial_i(u_1)_j + \partial_j(u_1)_i - \frac{2}{d}g_{ij}\partial_k u_1^k\right] + \frac{\zeta}{T_0}\big(\partial_k u_1^k\big)^2. \tag{108}$$

Then, restricting to one-dimensional motion and using our thermodynamic relations and first-order solutions, we find

$$\partial_\mu s^\mu = (\partial_x n_1)^2\left[\zeta + 2\eta\left(1-\frac{1}{d}\right)\right]\frac{v_0^2}{T_0 n_0^2} + O(\epsilon). \tag{109}$$

We see that entropy is generated at locations where the derivative of n_1 is largest: for solitons, this occurs at the leading and trailing faces (Fig. 3). Further, as the soliton spreads out, the entropy production slows over time (Fig. 4). Finally, for the Dirac regime, σ_Q-induced entropy production

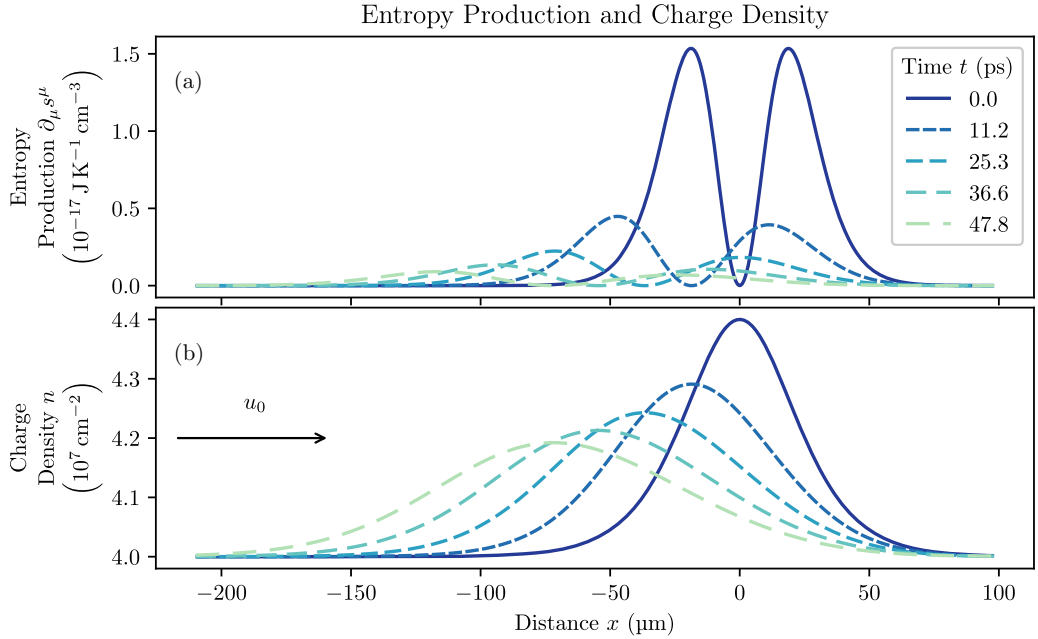

FIG. 3. The entropy production $\partial_\mu s^\mu$ (a) and soliton charge density n_1 (b) at select times. Values used were $\mathcal{A} = 0.88$, $\mathcal{B} = -0.70$, $\mathcal{C} = -0.060$, $\mathcal{F} = -1.1$, and $\mathcal{G} = 0.53$ with the height normalized to $4.0 \times 10^8\,\mathrm{cm}^{-2}$.

is suppressed to subleading order; η and ζ are the main producers of entropy.

VII. EXPERIMENTAL PROPOSAL

Here, we will briefly detail the applicability of this theory to experiment.

A. Values of parameters

It has been more convenient to deal with nondimensional variables throughout the derivation. However, we now convert back to dimensionful quantities to better understand their physical magnitude. It is worth emphasizing that this conversion is dependent on the nondimensionalization we chose. The values calculated in this section are specific to the Dirac regime nondimensionalization laid out in Sec. III; a similar analysis could be performed for the Fermi regime nondimensionalization specified in Appendix B 1.

The dimensional and nondimensional values of the various parameters in the problem are listed in Table I. For the remainder of this section, we will specialize to dimension $d = 2$. Note that we are using the values $v_F = c/300$ [1] and $l_{\mathrm{ref}} = 50\,\mathrm{nm}$. For computing the sample values, we have chosen $\epsilon = 0.1$. We see that all of the nondimensional parameters are approximately equal to unity, as required. However, there are a few points to note.

In previous experiments, the distance between the graphene and the gates d_i $(i = 1, 2)$ was usually on the order of 300 nm [45]. We require a larger gate distance of

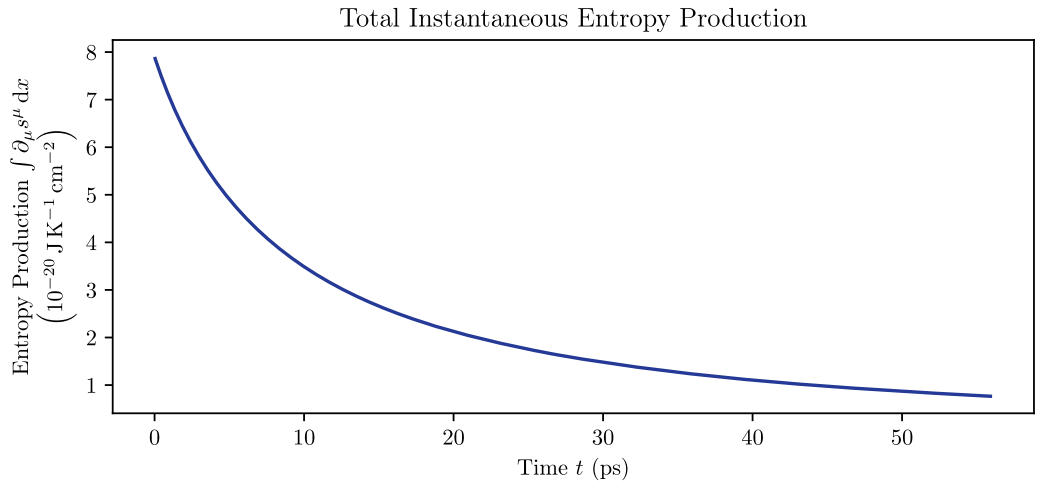

FIG. 4. The instantaneous entropy production $\partial_\mu s^\mu$ as a function of time. Values used were $\mathcal{A} = 0.88$, $\mathcal{B} = -0.70$, $\mathcal{C} = -0.060$, $\mathcal{F} = -1.1$, and $\mathcal{G} = 0.53$ with the height normalized to $4.0 \times 10^8\,\mathrm{cm}^{-2}$.

TABLE I. Values of the various parameters in terms of the small parameter ϵ. Sample values are given for $\epsilon = 0.1$ and dimension $d = 2$.

	ϵ-dependence	Sample Nondim. value	Sample Dim. value
n_0	$\epsilon\hat{n}_0\ 4 \times 10^{10}\,\mathrm{cm}^{-2}$	1.0	$4.0 \times 10^{9}\,\mathrm{cm}^{-2}$
d_i	$\epsilon^{-5/4}\hat{d}_i\ 50\,\mathrm{nm}$	1.0	890 nm
A	$\epsilon^{-5/4}\hat{A}\ 5.3 \times 10^{-36}\,\mathrm{J\,m}^2$	0.22	$2.1 \times 10^{-35}\,\mathrm{J\,m}^2$
T_0	$\epsilon^{1/4}\hat{T}_0\ 150\,\mathrm{K}$	0.70	60 K
P_0	$\epsilon^{3/4}\hat{T}_0^3\ 8.4 \times 10^{-7}\,\mathrm{N\,m}^{-1}$	$1.1\ \hat{T}_0^3$	$5.9 \times 10^{-8}\,\mathrm{N\,m}^{-1}$
μ_0	$\epsilon^{3/4}\frac{\hat{n}_0}{\hat{T}_0}\ 2.1 \times 10^{-21}\,\mathrm{J}$	$1.1\ \frac{\hat{n}_0}{\hat{T}_0}$	$6.1 \times 10^{-22}\,\mathrm{J}$
σ_Q	$\epsilon^{1/2}\hat{\sigma}_Q\ 0.24\,\mathrm{k\Omega}^{-1}$	0.63	$0.048\,\mathrm{k\Omega}^{-1}$
η	$\hat{\eta}\ 4.2 \times 10^{-20}\,\mathrm{kg\,s}^{-1}$	1.1	$4.8 \times 10^{-20}\,\mathrm{kg\,s}^{-1}$

$d_i = 890\,\mathrm{nm}$ corresponding to $\hat{d}_i = 1.0$. The static dielectric constant κ must be chosen relative to d_1 and d_2. For the remaining normalizations to be consistent, we require $\kappa \approx 1$. That is, the graphene should be suspended from its contacts with vacuum filling the gap between the graphene sheet and the conducting gates.

It is important to reiterate the way we nondimensionalized the intrinsic conductivity. At a temperature of 60 K, σ_Q/e^2 has a fixed value of $0.20\hbar^{-1}$. We needed to relate the relative sizes of nondimensional parameters ϵ and $\sigma_Q\hbar/e^2$ to solve the problem. Our derivation assumed $\epsilon \sim 0.1$, so that $\epsilon^{1/2} \sim \sigma_Q\hbar/e^2$. This fixes the value of $\hat{\sigma}_Q$ as $\hat{\sigma}_Q = 0.20\epsilon^{-1/2}$.

Notice that if ϵ is increased, then the numerical value of $\hat{\sigma}_Q$ decreases; hence, the intrinsic conductivity becomes a higher-order correction and drops out of our first-order solutions. Conversely, if ϵ is decreased, $\hat{\sigma}_Q$ could grow large and require a different nondimensionalization for σ_Q. For ϵ small enough, it would be more appropriate to take $\sigma_Q = \epsilon^0\hat{\sigma}_Q e^2/\hbar$. This alternative would require different nondimensionalizations for all variables (cf., Appendix B); nevertheless, similar solutions would result (though the viscosity would no longer appear in the first-order corrections). Similar considerations also apply for η, though it is considerably simpler given that $\eta l_{\mathrm{ref}}^d/\hbar \approx 1$.

It is also useful to determine the values of the parameters appearing as coefficients in the KdV and KdV-Burgers equations (i.e., $\mathcal{A}$, $\mathcal{B}$, $\mathcal{C}$, and $\mathcal{G}$). For instance, consider the case with $v_0 = 0$, $u_0 > 0$, and $U_1 = 0$; we will also set $\zeta = 0$ and choose $c_1 = 1.0$. Using the above values and the bare thermodynamic coefficients $\mathcal{C}_0$ and $\mathcal{C}_1$ (cf., Appendix A), we find $\mathcal{A} = 0.88$, $\mathcal{B} = -0.70$, $\mathcal{C} = -0.060$, $\mathcal{F} = -1.1$, and $\mathcal{G} = 0.53$ (cf., Fig. 1). Importantly, we see that $\mathcal{B}$, $\mathcal{C}$, and $\mathcal{G}$ are all roughly the same order, implying that nonlinearity, dispersion, and dissipation are equally important.

B. Source and signal

As we discussed in Sec. III, the characteristic length of the disturbance ξ is related to l_{ref} as $\xi = l_{\mathrm{ref}}/\epsilon^{(d+5)/4}$. For $d = 2$ and $\epsilon = 0.1$ with graphene's $l_{\mathrm{ref}} = 50\,\mathrm{nm}$, we find a pulse width of approximately 2.8 μm. For the $u_0 = 0$ case, the propagation speed is approximately $v = 0.43v_F \sim 0.43c/300$, giving a bandwidth of roughly $v/\xi = 150\,\mathrm{GHz}$.

If we consider the stationary soliton case $v_0 = 0$, we need to source a background current $u_0 \neq 0$ to counteract its propagation. In Sec. IV, we found that $u_0 = 0.40\,v_F = 4.0 \times 10^5\,\mathrm{ms}^{-1}$; with a charge density of $n_0 = 4.0 \times 10^9\,\mathrm{cm}^{-2}$, we need a current density of $K_0 = |en_0u_0| = 2.5\,\mathrm{Am}^{-1}$.

As shown previously, the system has a (dimensional) characteristic decay time of

$$t_d = \frac{45 l_{\mathrm{ref}}\mathcal{A}|\mathcal{C}|}{4\epsilon^{11/4}v_F\mathcal{G}|\mathcal{B}|}. \tag{110}$$

Inserting the previously chosen values for these coefficients, we find $t_d \approx 44$ ps.

To estimate the magnitude of the signal, we first calculate the background chemical potential $\mu_0 = \epsilon^{3/4}\hbar v_F l_{\mathrm{ref}}^{-1}\hat{\mu}_0 = 6.1 \times 10^{-22}$ J. From this, we find the background voltage $V_0 = \mu_0/e = 3.8$ mV. Then, the signal voltage $V_1 = \mu_1/e$ would be a factor of $\epsilon \sim 0.1$ smaller, or 380 μV.

C. Joule heating

For the nonpropagating case ($v_0 = 0$), a large uniform background current u_0 flows through the graphene; this will cause Joule heating of the entire sample due to graphene's resistance. It is worthwhile to verify that this heating occurs sufficiently slowly so as not to interfere with the soliton's propagation and decay.

The power produced, per unit area, by Joule heating is

$$P_J = K_0^2\rho, \tag{111}$$

with resistivity ρ and surface current density K_0. As a worst-case scenario, assuming the graphene does not lose any heat to the environment, this power goes solely toward heating the graphene.

The specific heat of graphene [46] at 60 K is approximately $60\,\mathrm{mJ\,g}^{-1}\,\mathrm{K}^{-1}$. Given an atomic mass of $12.01\,\mathrm{g\,mol}^{-1}$ for carbon and an atomic density of $6.3\,\mathrm{mol\,cm}^{-2}$ for carbon atoms in graphene [47], we find a specific heat of $c_s = 4.5 \times 10^{-9}\,\mathrm{J\,cm}^{-2}\mathrm{K}^{-1}$.

Therefore, the soliton's temperature will change at a rate of $P_J/c_s = 3.0\,\mathrm{K\,ns}^{-1}$. Given that the suggested experiment would be measuring the soliton's temperature anomaly $T_1 = \epsilon T_0$, it would only be sensitive to Joule heating after a temperature change of similar magnitude had been generated. Hence, it would take approximately $T_1c_s/P_J = 2.0$ ns for the system

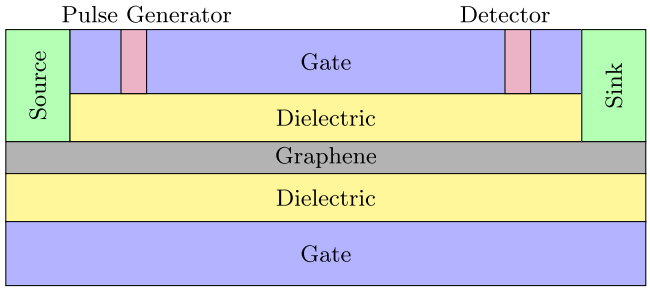

FIG. 5. Side view of the proposed experimental setup; the graphene is sandwiched between two layers of dielectric, and further sandwiched between two conducting gates. A source and sink on either edge of the graphene generate the background current u_0. The pulse generator produces the soliton, and the detector detects it.

to heat appreciably. Given that this time is long compared to the characteristic timescales of the problem (t_{char} and t_d), we are justified in neglected Joule heating.

Notice that the characteristic Joule-heating time is also long compared to the electron-phonon scattering time; this implies the electrons and graphene lattice would thermalize relatively quickly compared to the Joule heating time. This is why we utilized the specific heat of the entire graphene system (electrons and lattice) as opposed to the specific heat of only the electrons.

D. Experimental setup

The solitonic solutions we have derived offer a means to experimentally measure the viscosity η of graphene. In particular, the viscous coefficients σ_Q, η, and ζ all enter into the coefficient we have denoted $\mathcal{G}$. Therefore, if the value of $\mathcal{G}$ can be measured, then the viscosity can be determined.

Referring to the expression for $\mathcal{G}$, we see that η only appears in the combination $\zeta + 2\eta(1 - 1/d)$; hence, it is this quantity that can be determined from experiment. In practice, we expect $\zeta \ll \eta$, and thus this procedure offers an estimate for η [1]. Furthermore, determining η from $\mathcal{G}$ requires knowing the values of all the other parameters P_0, n_0, etc. Most of these are experimentally determined and hence known; the only other necessary quantity is the intrinsic conductivity σ_Q. Previous measurements of this quantity exist [4,5]; therefore, it can be treated as a known quantity.

An initial disturbance needs to be generated in the graphene; for instance, this can be accomplished via a short voltage spike produced by a thin contact placed laterally atop the sample (cf., Fig. 5). It is well known that the KdV equation causes a localized profile to split into a series of left- and right-moving solitons [48] sorted by height. After the disturbance is allowed to propagate a sufficient distance, the individual solitons should have separated enough to be separately distinguished. The actual population of solitons generated by the pulse will be dependent on the contact's shape and voltage profile: the distribution of soliton heights and widths can be determined by the inverse scattering transform [49].

Given that the solitons represent a localized change in the charge density, it should be possible to detect them with a voltmeter; a voltage time-series could then reconstruct the soliton profile. The dissipative terms cause two measurable effects: a change in the propagation speed and a decay of the soliton's height. This requires measuring either the soliton's speed or amplitude as a function of time. Depending on the particular experimental setup, one effect might be more accessible than the other. Next, we describe two possible experimental setups.

1. No propagation

Without a background current $u_0 = 0$, the soliton propagates at a speed $v \approx v_F \approx c/300$. Such a fast propagation speed could make measurement difficult. One way to mitigate this is to impose a countercurrent u_0 in the opposite direction of propagation; as detailed in Sec. IV, it is possible to choose a background current $u_0 + \epsilon U_1$ such that the soliton is stationary in the laboratory frame $v_0 + \epsilon v_1 = 0$. Doing this should make obtaining the height measurements much easier. In fact, the speed measurements are still feasible in this setup since the dissipation causes v_1, and hence the control current U_1, to decay over time.

One possible barrier to implementation of this method is the boundary condition of graphene. So far, we have neglected boundary effects by assuming one-dimensional propagation; depending on graphene's boundary conditions, this might not be justified. Graphene most likely satisfies one of two possible boundary conditions [50]: either a no-slip boundary ($\mathbf{u} = \mathbf{0}$) or no-stress (no normal velocity gradient, i.e., $[\hat{n} \cdot \nabla]\mathbf{u} = \mathbf{0}$ with $\hat{n}$ the boundary unit normal). If the actual boundary is no-slip, our one-dimensional propagation assumption is violated; in this case, the sample must be sufficiently wide to ignore edge effects, or a different experimental setup (cf., the next section) is needed. Conversely, a no-stress boundary permits our one-dimensional soliton solution. There is some experimental evidence that no-stress boundaries are the correct boundary type [1], and theory predicts that weakly disordered edges at low temperature ($T \lesssim 40\,\text{K}$) have a slip-length on the order of 50 μm. Therefore, it is plausible that, for graphene samples of width at most $\sim$100 μm, a no-stress boundary condition is appropriate, allowing for large u_0 countercurrent.

2. No background current

If graphene instead possesses a no-slip boundary condition, a different experimental method will be needed. For this setup, we will not use a background flow, $u_0 = 0$. Then, the boundary conditions are mostly irrelevant, since the fluid velocity is now of order $O(u_1) = \epsilon v_F$ and can therefore be made small. For this setup, height measurements are more suitable; after one decay period τ_0, the height decreases by a factor of $\frac{1}{2}$ while the propagation velocity changes by a factor of $\delta v/v_0 = \frac{1}{2}\epsilon \ll 1$.

Following the method proposed by Coelho *et al.* [51], we recommend periodically producing a voltage pulse and measuring a set distance away. By averaging over many realizations, it should be possible to obtain a wave profile. This could be repeated at a few locations, thereby measuring the decay rate as a function of downstream position.

This method is likely more difficult experimentally given that it requires taking measurements at multiple locations

sequentially. However, it has the benefit of being theoretically sound regardless of graphene's boundary conditions.

VIII. CONCLUSION

Graphene offers a fantastic environment for studying strong-coupling phenomena. Hydrodynamic analysis presents a useful set of tools for analyzing the long-wavelength physics in such a clean, strongly coupled system. The Fermi liquid regime has much in common with ordinary metals and has been the focus of many experiments in graphene; meanwhile, the Dirac fluid regime hosts a number of intriguing phenomena. When graphene is placed in a hydrodynamic regime, the electrons obey relativistic Navier-Stokes equations and can form solitonic solutions. An ordinary perturbation expansion was used to derive the special case of a stationary soliton on a background counterflow. Additionally, a full multiple scales asymptotic analysis was utilized to treat the general case with arbitrary background flow. These methods furnished analytic approximations to the shape and speed of the predicted solitons. This analysis did not deal with the boundary conditions of the fluid flow; this offers an interesting avenue for future research.

By including dissipation in our system, we were able to model the decay of the solitons. The analysis showed that dissipation causes both a decay of the soliton's height as well as its speed. This decay rate offers a means to experimentally measure dissipation in the hydrodynamic regime of graphene. The results of this paper help elucidate the connection between solitons in the Fermi and Dirac regimes of graphene and put forward a new method for measuring hydrodynamically relevant parameters such as the intrinsic conductivity and shear viscosity.

ACKNOWLEDGMENTS

Special thanks go to Falk Feddersen for his invaluable support and input. The computations in this paper were performed using MAPLE™ [52]. This work was supported in part by funds provided by the US Department of Energy (DOE) under cooperative research agreement DE-SC0009919.

APPENDIX A: THERMODYNAMIC COEFFICIENTS

Following Lucas and Fong [1], we can derive the pressure for weak coupling, starting from the grand-canonical ensemble for a free Fermi gas in d dimensions,

$$\begin{aligned} P(\mu,T) &= -\frac{\Phi_G}{V} \\ &= \frac{k_BT}{V}\sum_{A,\mathbf{p}}\ln(\mathcal{Z}_{A,\mathbf{p}}) \\ &= k_BT\sum_A\int\frac{d^d\mathbf{p}}{(2\pi\hbar)^d}\ln(1+e^{[q_A\mu-\varepsilon_A(\mathbf{p})]/k_BT}) \\ &= -\frac{4(k_BT)^{d+1}\Omega_{d-1}(d-1)!}{(2\pi\hbar v_F)^d}[\mathrm{Li}_{d+1}(-e^{\mu/k_BT}) \\ &\quad +\mathrm{Li}_{d+1}(-e^{-\mu/k_BT})]. \end{aligned} \tag{A1}$$

Here, we have Φ_G the grand potential, $\mathcal{Z}=\exp(-\Phi_G/k_BT)$ the grand partition function, and V the volume. We made use of the fact that, for a free Fermi gas, the grand partition function is separable over modes (A and $\mathbf{p}$): $\mathcal{Z}=\prod_{A,\mathbf{p}}\mathcal{Z}_{A,\mathbf{p}}$. Additionally, we have the excitation energy $\varepsilon_A(\mathbf{p})=v_F|\mathbf{p}|$, $\Omega_{d-1}=2\pi^{d/2}/\Gamma(d/2)$ the surface area of a unit $(d-1)$-sphere, Γ is the gamma function, and Li_d the polylogarithm of order $d+1$. Note that the sum over species runs over spin/valley degeneracy (giving a factor of 4) as well as electrons/holes with $q_A=\pm1$. More specifically, $\sum_A\ln(\mathcal{Z}_A)=4\ln(\mathcal{Z}_1(\mu,T))+4\ln(\mathcal{Z}_1(-\mu,T))$.

Likewise, the carrier density is given by

$$\begin{aligned} n(\mu,T) &= \frac{\partial P}{\partial\mu} \\ &= \frac{4(k_BT)^d\Omega_{d-1}(d-1)!}{(2\pi\hbar v_F)^d} \\ &\quad\times[-\mathrm{Li}_d(-e^{\mu/k_BT})+\mathrm{Li}_d(-e^{-\mu/k_BT})]. \end{aligned} \tag{A2}$$

We can develop series (asymptotic) expansions in Dirac (Fermi) regimes.

In the Dirac regime ($\mu\ll k_BT$), the polylogarithm can be approximated as [53]

$$\mathrm{Li}_s(-e^z)=-\sum_{k=0}^{\infty}\eta(s-k)\frac{z^k}{k!} \tag{A3}$$

for $|z|<\pi$, with η the Dirichlet eta function. Thus, the pressure is given by

$$\begin{aligned} P(\mu,T) &= 8\frac{(k_BT)^{d+1}\Omega_{d-1}(d-1)!}{(2\pi\hbar v_F)^d} \\ &\quad\times\sum_{k=0}^{\infty}\frac{\eta(d+1-2k)}{(2k)!}\left(\frac{\mu}{k_BT}\right)^{2k} \\ &= 8\frac{(k_BT)^{d+1}\Omega_{d-1}(d-1)!}{(2\pi\hbar v_F)^d}\Bigg[\eta(d+1) \\ &\quad+\frac{\eta(d-1)}{2}\left(\frac{\mu}{k_BT}\right)^2+O\left(\frac{\mu}{k_BT}\right)^4\Bigg], \end{aligned} \tag{A4}$$

and the carrier density is

$$\begin{aligned} n(\mu,T) &= \frac{8\mu(k_BT)^{d-1}\Omega_{d-1}(d-1)!}{(2\pi\hbar v_F)^d} \\ &\quad\times\sum_{k=0}^{\infty}\frac{\eta(d-1-2k)}{(2k+1)!}\left(\frac{\mu}{k_BT}\right)^{2k} \\ &= \frac{8\mu(k_BT)^{d-1}\Omega_{d-1}(d-1)!}{(2\pi\hbar v_F)^d}\Bigg[\eta(d-1) \\ &\quad+\frac{\eta(d-3)}{6}\left(\frac{\mu}{k_BT}\right)^2+O\left(\frac{\mu}{k_BT}\right)^4\Bigg]. \end{aligned} \tag{A5}$$

For instance, for $d=2$, we find

$$P=\frac{(k_BT)^3}{(\hbar v_F)^2}\left[\frac{4\eta(3)}{\pi}+\frac{2\ln(2)}{\pi}\left(\frac{\mu}{k_BT}\right)^2+O\left(\frac{\mu}{k_BT}\right)^4\right] \tag{A6}$$

and

$$n = \frac{\mu(k_B T)}{(\hbar v_F)^2}\left[\frac{4\ln(2)}{\pi} + \frac{1}{6\pi}\left(\frac{\mu}{k_B T}\right)^2 + O\left(\frac{\mu}{k_B T}\right)^6\right]. \quad \text{(A7)}$$

Instead, in the Fermi regime ($\mu \gg k_B T$), an asymptotic expansion of the polylogarithm is given by [53]

$$\mathrm{Li}_s(-e^z) = -2\sum_{k=0}^{\lfloor s/2\rfloor}\frac{\eta(2k)}{(s-2k)!}(z)^{s-2k} + O(e^{-z}) \quad \text{(A8)}$$

for $\mathrm{Re} z \gg 1$, while $\mathrm{Li}_s[-\exp(-z)]$ is subdominant and therefore can be neglected. Thus, we find

$$\begin{aligned} P(\mu, T) &= \frac{8|\mu|^{d+1}\Omega_{d-1}}{(2\pi\hbar v_F)^d}\sum_{k=0}^{\lfloor (d+1)/2\rfloor}\frac{\eta(2k)(d-1)!}{(d+1-2k)!}\left(\frac{k_B T}{\mu}\right)^{2k} \\ &= \frac{8|\mu|^{d+1}\Omega_{d-1}}{(2\pi\hbar v_F)^d}\left[\frac{1}{2(d+1)d} + \frac{\pi^2}{12}\left(\frac{k_B T}{\mu}\right)^2 \right. \\ &\quad \left. + O\left(\frac{k_B T}{\mu}\right)^4\right], \end{aligned} \quad \text{(A9)}$$

and the carrier density is

$$\begin{aligned} n(\mu, T) &= \frac{8|\mu|^d \mathrm{sgn}(\mu)\Omega_{d-1}}{(2\pi\hbar v_F)^d}\sum_{k=0}^{\lfloor d/2\rfloor}\frac{\eta(2k)(d-1)!}{(d-2k)!}\left(\frac{k_B T}{\mu}\right)^{2k} \\ &= \frac{8|\mu|^d \mathrm{sgn}(\mu)\Omega_{d-1}}{(2\pi\hbar v_F)^d}\left[\frac{1}{2d} + \frac{\pi^2(d-1)}{12}\left(\frac{k_B T}{\mu}\right)^2 \right. \\ &\quad \left. + O\left(\frac{k_B T}{\mu}\right)^4\right]. \end{aligned} \quad \text{(A10)}$$

Again, for $d = 2$, we have

$$P = \frac{|\mu|^3}{(\hbar v_F)^2}\left[\frac{1}{3\pi} + \frac{\pi}{3}\left(\frac{k_B T}{\mu}\right)^2 + O\left(\frac{k_B T}{\mu}\right)^4\right] \quad \text{(A11)}$$

and

$$n = \frac{\mu^2 \mathrm{sgn}(\mu)}{(\hbar v_F)^2}\left[\frac{1}{\pi} + \frac{\pi}{3}\left(\frac{k_B T}{\mu}\right)^2 + O\left(\frac{k_B T}{\mu}\right)^4\right]. \quad \text{(A12)}$$

Thus, we find the following coefficients:

$$\mathcal{C}_0^F = \frac{8|\mu|^{d+1}\Omega_{d-1}}{(2\pi\hbar v_F)^d}\frac{1}{2(d+1)d}, \quad \text{(A13)}$$

$$\mathcal{C}_1^F = \frac{8|\mu|^{d+1}\Omega_{d-1}}{(2\pi\hbar v_F)^d}\frac{\pi^2}{12}, \quad \text{(A14)}$$

and

$$\mathcal{C}_0^D = 8\frac{(k_B T)^{d+1}\Omega_{d-1}(d-1)!}{(2\pi\hbar v_F)^d}\eta(d+1), \quad \text{(A15)}$$

$$\mathcal{C}_1^D = 8\frac{(k_B T)^{d+1}\Omega_{d-1}(d-1)!}{(2\pi\hbar v_F)^d}\frac{\eta(d-1)}{2}. \quad \text{(A16)}$$

When screening is not negligible, these coefficients get renormalized. For instance, the Dirac coefficients for $d = 2$ and $T \to 0$ become [54]

$$\mathcal{C}_0^D = 8\frac{(k_B T)^3\Omega_1}{(2\pi\hbar v_F)^2}\eta(3)\left(\frac{\alpha(T)}{\alpha_0}\right)^2, \quad \text{(A17)}$$

$$\mathcal{C}_1^D = 8\frac{(k_B T)^3\Omega_1}{(2\pi\hbar v_F)^2}\frac{\eta(1)}{2}\left(\frac{\alpha(T)}{\alpha_0}\right)^2, \quad \text{(A18)}$$

with $\alpha(T)$ given in Eq. (26).

APPENDIX B: GENERAL NONDIMENSIONALIZATION

A critical aspect of these derivations was the correct choice of nondimensionalization scheme. Depending on the physical regime of interest (Fermi versus Dirac) as well as the relative size of terms (e.g., how large ϵ is compared to $\sigma_Q\hbar/e^2$), different nondimensionalization choices may be appropriate. To elucidate the relationship between these various schemes, a single, general nondimensionalization can be performed. In this Appendix, we will use a unit system in which $\hbar = v_F = k_B = l_{\mathrm{ref}} = e = 1$. Note: we are only nondimensionalizing ($\hbar = 1$, etc.), but not normalizing; i.e., we are not requiring that all quantities are unity (unlike the quantities denoted earlier by carets).

For convenience, the main results are collected here:

$$\begin{aligned} O(\mu) &= \epsilon^{\frac{1}{2}q-\frac{1}{2}p+\frac{1}{2}m+\frac{1}{2}|m|}\sqrt{\frac{O(\eta)}{O(\sigma_Q)}}, \\ O(T) &= \epsilon^{\frac{1}{2}q-\frac{1}{2}p+\frac{1}{2}|m|}\sqrt{\frac{O(\eta)}{O(\sigma_Q)}}, \\ O(P) &= \epsilon^{\frac{d+1}{2}q-\frac{d+1}{2}p+\frac{d+1}{4}m+\frac{d+1}{4}|m|}\sqrt{\frac{O(\eta)}{O(\sigma_Q)}}^{d+1}, \\ O(n) &= \epsilon^{\frac{d}{2}q-\frac{d}{2}p+\frac{d+1}{4}m+\frac{d+1}{4}|m|}\sqrt{\frac{O(\eta)}{O(\sigma_Q)}}^{d}, \\ O(\partial_x) &= \epsilon^{1+\frac{d+1}{2}q-\frac{d-1}{2}p+\frac{d+1}{4}m+\frac{d+1}{4}|m|}\sqrt{\frac{O(\eta)^{d-1}}{O(\sigma_Q)^{d+1}}}, \\ O(d_i) &= \epsilon^{-\frac{1}{2}-\frac{d+1}{2}q+\frac{d-1}{2}p-\frac{d+1}{4}m-\frac{d+1}{4}|m|}\sqrt{\frac{O(\sigma_Q)^{d+1}}{O(\eta)^{d-1}}}, \\ O(u) &= 1, \\ O(A) &= \epsilon^{\frac{-d+1}{2}q+\frac{d-1}{2}p-\frac{d+1}{4}m-\frac{d+1}{4}|m|}\sqrt{\frac{O(\sigma_Q)}{O(\eta)}}^{d-1}. \end{aligned} \quad \text{(B1)}$$

Here, we have defined four parameters [55]: d the spatial dimension, $m \in \mathbb{Z} \setminus \{0\}$, $p \in \mathbb{N} \geqslant 0$, and $q \in \mathbb{N} \geqslant 0$. The parameter m is defined as

$$\epsilon^m := O\left(\frac{\mu}{k_B T}\right)^2, \quad \text{(B2)}$$

and it represents the "Dirac" or "Fermi" quality of the system: $m > 0$ corresponds to increasingly strong "Dirac" character while $m < 0$ is more "Fermi"-like. The parameter p measures the importance of the shear terms η: if $p = 0$, the shear terms

enter our first-order correction equations while, for $p > 0$, it enters at the $(p+1)$-order correction equations and thus is not considered in our analysis. Likewise, the parameter q measures the importance of the conductive terms σ_Q: if $q = 0$, the conductive terms enter our first-order correction equations, but they are higher order for $q > 0$.

The KdV-Burgers coefficients specified in Appendixes E and F and throughout the paper assume $p = q = 0$. When using other choices of p and q, it is important to replace $\eta \to \eta\delta_{p,0}$, $\zeta \to \zeta\delta_{p,0}O(\zeta)/O(\eta)$, and $\sigma_Q \to \sigma\delta_{q,0}$. This ensures that only the relevant dissipative coefficients appear.

Note that we have specified $O(u) = 1$ to allow for large background flows $O(u_0) = 1$. Nevertheless, these results still apply if $u_0 = 0$ (no background flow), in which case $u \sim \epsilon u_1$ and $O(u) = \epsilon$. Additionally, these nondimensionalizations assume that $u < 1$ is small enough that $\gamma = 1/\sqrt{1-u^2}$ is order $O(\gamma) = 1$. Finally, note that we have assumed $O(\eta) \geqslant O(\zeta)$.

1. Parameter choice

For concreteness, the main paper utilizes a Dirac regime nondimensionalization of $m = 1$ and $p = q = 0$ with $O(\eta) = 1$ and $O(\sigma_Q) = \epsilon^{1/2}$.

We also highlight additional terms in the multiple scales expansion arising from the Fermi regime. These come about from a nondimensionalization with $m = -1$ and $p = q = 0$ with $O(\eta) = O(\sigma_Q) = 1$.

The alternate derivation for small ϵ mentioned in Sec. VII would correspond to $m = p = 1$ and $q = 0$ with $O(\eta) = O(\sigma_Q) = 1$.

It is worth highlighting that different choices of $O(\sigma_Q)$ and $O(\eta)$ do not affect the calculated results or observables (cf., Appendix B 3). Likewise, the parameters m, p, and q have minimal, straightforward effects on the results: p determines whether η and ζ terms appear in $\mathcal{G}'$; q determines if σ_Q appears in $\mathcal{G}'$; and m determines the form of P_1, and thus $\mathcal{F}'$ [56]. Otherwise, the results are independent of the choice of m, p, and q. To wit, these choices do not even affect the ϵ-order of observable quantities; see Section VI.

Using the definition of A, it is easy to check that $\kappa \geqslant 1$ satisfies $O(\kappa) = \epsilon^{-1/2-q}O(\sigma_Q)O(\alpha) \geqslant 1$; this provides a constraint on the allowed parameters. For $\epsilon = 0.1$, $q = 0$, $O(\sigma_Q) = \epsilon^{1/2}$, and $O(\alpha) = 1$ used throughout the main text, we find $O(\kappa) = 1$, consistent with our choice of $\kappa = 1$.

2. Entropy divergence

In Sec. VI C, we found that the entropy divergence only depended on the η and ζ terms, to this order. Using our expressions for the generalized nondimensionalization, we can investigate what occurs for different parameter regimes.

Recall that Eq. (107) showed that

$$O(\partial_\nu s^\nu) = \frac{1}{O(T)}O(\partial_x u)^2[O(\eta) + O(\zeta)] + \frac{O(\sigma_Q)}{O(T)}[O(\partial_x \mu) + O(F^{x\rho}u_\rho)]^2. \tag{B3}$$

Restricting our attention, as usual, to $u < 1$ such that $\gamma = 1/\sqrt{1-u^2} \approx 1$, we see that $O(F_{i\rho}u^\rho) = O(E_x) = O(\partial_x\phi) = O(\partial_x An)$. Thus, using the results from Appendix B, we have

$$O(\partial_\nu s^\nu) = \frac{O(\eta)O(\partial_x)^2\epsilon^{2-p}}{O(T)}\left[\epsilon^p + \frac{O(\zeta)}{O(\eta)}\epsilon^p + \epsilon^q + \epsilon^{q+\frac{1}{2}m+\frac{1}{2}|m|} + \epsilon^{q+m+|m|}\right]. \tag{B4}$$

Here, the terms in the square brackets represent the η, ζ, $\sigma_Q E_x^2$, $\sigma_Q E_x\partial_x\mu$, and $\sigma_Q(\partial_x\mu)^2$ terms, respectively. Hence, we recognize that increasing p causes the η and ζ terms to be less relevant, while increasing q does the same to the σ_Q terms. Furthermore, the leading factor of μ/T for the σ_Q terms in Eq. (107) causes these terms to be higher order when $m > 0$ (i.e., when μ/T is small), as expected. Finally, note that Eqs. (B1) were defined under the assumption $O(\eta) \geqslant O(\zeta)$, so $O(\zeta)/O(\eta)$ in Eq. (B4) can be, at most, unity.

3. Order of dissipative coefficients

Notice that we have left $O(\sigma_Q)$ and $O(\eta)$ undetermined. There is some subtlety in choosing these parameters. This most obvious manner to proceed involves using existing theoretical predictions [1] for their magnitude [57]; for instance, in $d = 2$,

$$\eta \approx \begin{cases} \frac{0.45T^2}{\alpha^2} & \text{Dirac,} \\ \frac{3\mu^2|n|}{64\pi\alpha^2\ln(\alpha^{-1})T^2} & \text{Fermi,} \end{cases} \tag{B5}$$

and

$$\sigma_Q = \begin{cases} \frac{0.12}{\alpha^2} & \text{Dirac,} \\ 1 & \text{Fermi,} \end{cases} \tag{B6}$$

with $\alpha \approx 4/\ln(10^4\,\mathrm{K}/T)$. Ignoring logarithmic corrections, these will then generate compatibility conditions on the parameters m, p, and q. Nevertheless, such a choice is only valid in the infinitesimal ϵ limit: we must assume ϵ is small enough that all the numerical prefactors—like $3/64\pi \approx 0.015$ for η in the Dirac regime—are considered order-1 [i.e., $O(\epsilon^0)$]. If ϵ is large enough that, for instance, $3/64\pi \approx \epsilon$, then this assumption breaks down.

Alternatively, one could instead calculate the numerical values for σ_Q and η from the existing theories. For instance, in Sec. III, we calculated $\sigma_Q = 0.20$ for our choices of parameters. This value can then be compared to the expected value of ϵ to determine the correct scaling. Continuing our example, assuming $\epsilon \approx 0.1$, we found $\sigma_Q \approx \epsilon^{1/2}$. While this method is somewhat more ad hoc than the previously described one, it has the benefit that it is now valid in a neighborhood of the desired ϵ rather than for solely infinitesimal ϵ. This is the method used in the main text since we are considering ϵ small but finite.

4. Derivation: Dominant balance

Now, we will derive the results given at the beginning of Appendix B. These results follow from the application of dominant balance.

First, we define a small nondimensional parameter $\epsilon \ll 1$ as our expansion parameter: that is, all terms will be expanded in integer powers of ϵ as $y = y_0 + \epsilon y_1 + \cdots$. Further, we will assume that all leading-order quantities are uniform in space and constant in time [i.e., $y(x,t) = y_0 + \epsilon y_1(x,t) + \cdots$]. This

implies that derivatives will always generate one extra factor of ϵ: $O(\partial_\mu y(x,t)) = O(\partial_\mu \epsilon y_1(x,t)) = \epsilon O(\partial_\mu) O(y)$.

Next, we introduce the parameter $m \in \mathbb{Z} \setminus \{0\}$ as

$$\epsilon^m := O\left(\frac{\mu}{T}\right)^2. \tag{B7}$$

We require that m be an integer since it enters in an asymptotic expansion of the equation of state $P(\mu, T)$; since our main equations are expanded in integer powers of ϵ, we must also have this asymptotic expansion in integer powers of ϵ. Also, notice we used the square of μ/T; it is easily seen that the asymptotic expansion of $P(\mu, T)$ only involves even powers of μ/T since it is an even function of μ/T [58]. Thus, we see that the Dirac regime follows when $m > 0$ and the Fermi case corresponds to $m < 0$; the $m = 0$ case is excluded because then the thermodynamic equation of state [cf., Eq. (A1)] cannot be expanded in a series/asymptotic expansion.

With this definition, we are able to collapse the two different nondimensionalizations of the pressure. From the thermodynamic equation of state Eq. (A1), we see that $O(P) = O(T)^{d+1}$ for Dirac and $O(P) = O(\mu)^{d+1}$ for Fermi. Therefore, we have $O(P) = \epsilon^{(d+1)m/4+(-d-1)|m|/4} O(T)^{d+1}$ in general. Likewise, the charge density can be nondimensionalized as $O(n) = \epsilon^{|m|/2} O(P)/O(T) = \epsilon^{(d+1)m/4+(-d+1)|m|/4} O(T)^d$.

Now, we begin using dominant balance to impose restrictions based on our desire that certain terms appear at certain orders. Here, we must use some foresight about which terms the equations will contain. To ensure that we have wavelike solutions, we want the terms appearing in the leading-order equations to match those in Sec. V. Since we want the dispersive electromagnetic terms $d_1 d_2 \partial_x^3 n$ to appear at first-order corrections, this means the nondispersive electromagnetic term $\partial_x n$ must appear at leading order. Thus, the two electromagnetic terms must differ by one factor of ϵ: this imposes $O(d_i) = \epsilon^{1/2}/O(\partial_x)$; this is our first assumption. Requiring the nondispersive electromagnetic term to enter at leading order enforces $O(\partial_x P) = O(An\partial_x n)$ yielding our second assumption: $O(A) = \epsilon^{(-d-1)m/4+(d-3)|m|/4} O(T)^{-d+1}$.

Next, we wish the leading-order equations to be satisfied even if $u_0 = 0$. Setting $u_0 = 0$ and performing a dominant balance on the leading charge conservation equation (74a) gives $O(\partial_t) = O(u)O(\partial_x)$, our third requirement. Another dominant balance on the leading momentum conservation equation (74b) yields $O(u) = 1$, our fourth and final requirement.

Moving onto the shear- and bulk-viscosity terms, we introduce a second parameter $p \in \mathbb{N} \geqslant 0$. This parameter is defined such that $p = 0$ ensures that the shear/bulk viscosities appear in our first-order correction equations, $p = 1$ would push these terms to second-order corrections, and so on. Since we are only concerned with first-order corrections, this means shear/bulk viscosity is relevant for $p = 0$ and irrelevant for $p > 0$. This is implemented by imposing $O(\epsilon \partial_x P) = \epsilon^{-p} O(\eta \partial_x^2 n)$, yielding $O(\partial_x) = \epsilon^{p+1} O(P)/O(\eta)$.

Finally, we introduce one more parameter $q \in \mathbb{N} \geqslant 0$ controlling the order at which the intrinsic conductivity σ_Q appears. Similar to the parameter p, the parameter $q = 0$ yields σ_Q terms at first-order while $q > 0$ corresponds to higher-order terms (which will be neglected in this analysis). It is easy to check that of the two σ_Q terms, the electromagnetic term $O(F^{\nu\rho} u_\rho) = O(A\partial_x n)$ is always larger than the thermoelectric term $O(T\partial_x(\mu/T)) \leqslant O(A\partial_x n)$. Thus, we introduce the parameter q as $O(\epsilon \partial_t n) = \epsilon^{-q} O(\sigma_Q \partial_x^2 A n)$. This implies that $O(T) = \epsilon^{q/2-p/2+|m|/2} \sqrt{O(\eta)/O(\sigma_Q)}$. Using these various relations reproduces the results given at the beginning of Appendix B.

APPENDIX C: ADIABATIC SYSTEM

Here, we can utilize the same nondimensionalization laid out in Appendix B for the isothermal system. This follows because the derivation in Appendix B 4 required that the leading-order equations still be satisfied when $u_0 = 0$. However, it is easy to show that, when $u_0 = 0$, the leading-order energy conservation equation (C15b) is equivalent to the leading-order charge conservation equation (C15a) combined with the isothermal relation between P and n. Thus, the leading order $u_0 = 0$ adiabatic system is equivalent to the leading order $u_0 = 0$ isothermal system, and the previous nondimensionalization carries over.

Here, we will redo the multiple scales derivation using the adiabatic assumption. Therefore, we will now include the energy conservation equation (10) and allow T to vary dynamically. As we did in Sec. V, we expand all of the dynamic variables (including T) in a perturbation expansion.

1. Perturbative thermodynamics

We will be using the thermodynamic relationships of Sec. II C to write μ and T in terms of n and P. Expanding the thermodynamic variables and collecting powers of ϵ yields the following relations for the Dirac regime:

$$P_0 = T_0^{d+1} \mathcal{C}_0, \tag{Dirac: C1}$$

$$n_0 = 2 T_0^{d-1} \mu_0 \mathcal{C}_1, \tag{Dirac: C2}$$

$$P_1 = P_0 \left[\frac{T_1}{T_0}(d+1) + \frac{\mathcal{C}_1}{\mathcal{C}_0} \left(\frac{\mu_0}{T_0}\right)^2 \delta_{m,1} \right], \tag{Dirac: C3}$$

$$n_1 = n_0 \left[\frac{\mu_1}{\mu_0} + \frac{T_1}{T_0}(d-1) + 2\frac{\mathcal{C}_2}{\mathcal{C}_1} \left(\frac{\mu_0}{T_0}\right)^2 \delta_{m,1} \right], \tag{Dirac: C4}$$

$$\begin{aligned} P_2 = P_0 \Bigg[& \frac{T_2}{T_0}(d+1) + \frac{T_1^2}{T_0^2}\frac{(d+1)d}{2} \\ & + \frac{\mathcal{C}_1}{\mathcal{C}_0}\left(2\frac{\mu_1}{\mu_0} + (d-1)\frac{T_1}{T_0}\right)\left(\frac{\mu_0}{T_0}\right)^2 \delta_{m,1} \\ & + \frac{\mathcal{C}_2}{\mathcal{C}_0}\left(\frac{\mu_0}{T_0}\right)^4 \delta_{m,1} + \frac{\mathcal{C}_1}{\mathcal{C}_0}\left(\frac{\mu_0}{T_0}\right)^2 \delta_{m,2} \Bigg], \end{aligned} \tag{Dirac: C5}$$

$$\begin{aligned} n_2 = n_0 \Bigg[& \frac{\mu_2}{\mu_0} + \frac{T_2}{T_0}(d-1) + \frac{T_1^2}{T_0^2}\frac{(d-1)(d-2)}{2} \\ & + \frac{\mu_1}{\mu_0}\frac{T_1}{T_0}(d-1) + 2\frac{\mathcal{C}_2}{\mathcal{C}_1}\left(3\frac{\mu_1}{\mu_0} + (d-3)\frac{T_1}{T_0}\right)\left(\frac{\mu_0}{T_0}\right)^2 \delta_{m,1} \\ & + 3\frac{\mathcal{C}_3}{\mathcal{C}_1}\left(\frac{\mu_0}{T_0}\right)^4 \delta_{m,1} + 2\frac{\mathcal{C}_2}{\mathcal{C}_1}\left(\frac{\mu_0}{T_0}\right)^2 \delta_{m,2} \Bigg]. \end{aligned} \tag{Dirac: C6}$$

Similarly, for the Fermi regime, we find

$$P_0 = |\mu_0|^{d+1}\mathcal{C}_0, \tag{Fermi: C7}$$

$$n_0 = |\mu_0|^d \mathrm{sgn}(\mu_0)\mathcal{C}_0(d+1), \tag{Fermi: C8}$$

$$P_1 = P_0\left[\frac{\mu_1}{\mu_0}(d+1) + \frac{\mathcal{C}_1}{\mathcal{C}_0}\left(\frac{T_0}{\mu_0}\right)^2\delta_{m,-1}\right], \tag{Fermi: C9}$$

$$n_1 = n_0\left[\frac{\mu_1}{\mu_0}d + \frac{\mathcal{C}_1}{\mathcal{C}_0}\frac{d-1}{d+1}\left(\frac{T_0}{\mu_0}\right)^2\delta_{m,-1}\right], \tag{Fermi: C10}$$

$$P_2 = P_0\left[\frac{\mu_2}{\mu_0}(d+1) + \frac{\mu_1^2}{\mu_0^2}\frac{(d+1)d}{2} + \frac{\mathcal{C}_1}{\mathcal{C}_0}\left(2\frac{T_1}{T_0} + (d-1)\frac{\mu_1}{\mu_0}\right)\left(\frac{T_0}{\mu_0}\right)^2\delta_{m,-1} + \frac{\mathcal{C}_2}{\mathcal{C}_0}\left(\frac{T_0}{\mu_0}\right)^4\delta_{m,-1} + \frac{\mathcal{C}_1}{\mathcal{C}_0}\left(\frac{T_0}{\mu_0}\right)^2\delta_{m,-2}\right], \tag{Fermi: C11}$$

$$\begin{aligned} n_2 = n_0\Bigg[&\frac{\mu_2}{\mu_0}d + \frac{\mu_1^2}{\mu_0^2}\frac{d(d-1)}{2} + \frac{\mathcal{C}_1}{\mathcal{C}_0}\frac{d-1}{d+1}\left(2\frac{T_1}{T_0} + (d-2)\frac{\mu_1}{\mu_0}\right)\left(\frac{T_0}{\mu_0}\right)^2\delta_{m,-1} \\ &+ \frac{\mathcal{C}_2}{\mathcal{C}_0}\frac{d-3}{d+1}\left(\frac{T_0}{\mu_0}\right)^4\delta_{m,-1} + \frac{\mathcal{C}_1}{\mathcal{C}_0}\frac{d-1}{d+1}\left(\frac{T_0}{\mu_0}\right)^2\delta_{m,-2}\Bigg]. \end{aligned} \tag{Fermi: C12}$$

In the Dirac regime, we can invert these relations to write μ and T in terms of P and n, treating these as the independent variables at each order. However, in the Fermi regime, this perturbation expansion introduces a peculiarity. The P_0 and n_0 equations do not contain T_0; therefore, rather than giving the value of T_0, these equations provide a constraint on P_0 and n_0:

$$P_0 = \frac{|n_0|^{(d+1)/d}}{|\mathcal{C}_0|^{1/d}(d+1)^{(d+1)/d}}\mathrm{sgn}C_0. \tag{Fermi: C13}$$

Similarly, the $P_1(x,t)$ and $n_1(x,t)$ equations only depend on a single dynamical variable $\mu_1(x,t)$ [but not $T_1(x,t)$]; therefore, these also give a restriction on P_1 and n_1 to ensure that $T_0(x,t) = T_0$ is independent of x and t:

$$\frac{P_1}{P_0} = \frac{n_1}{n_0}\frac{d+1}{d} + \frac{\mathcal{C}_1}{\mathcal{C}_0}\frac{1}{d}\left(\frac{T_0}{\mu_0}\right)^2\delta_{m,-1}. \tag{C14}$$

This requirement will be utilized later.

2. Conservation equations

If we again restrict to 1D motion and collect terms by powers of ϵ, we get the following equations:
Leading order:

$$\frac{\partial n_1}{\partial t_0} + \gamma^2 n_0 u_0\frac{\partial u_1}{\partial t_0} + u_0\frac{\partial n_1}{\partial x} + n_0\gamma^2\frac{\partial u_1}{\partial x} = 0, \tag{C15a}$$

$$\begin{aligned} &\gamma^2\frac{\partial \varepsilon_1}{\partial t_0} + \gamma^2 u_0^2\frac{\partial P_1}{\partial t_0} + 2u_0(\varepsilon_0+P_0)\gamma^4\frac{\partial u_1}{\partial t_0} + \left(1+u_0^2\right)(\varepsilon_0+P_0)\gamma^4\frac{\partial u_1}{\partial x} + u_0\gamma^2\frac{\partial}{\partial x}(\varepsilon_1+P_1) \\ &\qquad + An_0u_0\gamma^2\frac{\partial n_1}{\partial x} + An_0^2u_0^2\gamma^4\frac{\partial u_1}{\partial x} = 0, \end{aligned} \tag{C15b}$$

$$\gamma^3(\varepsilon_0+P_0)\frac{\partial u_1}{\partial t_0} + \gamma u_0\frac{\partial P_1}{\partial t_0} + u_0\gamma^3(\varepsilon_0+P_0)\frac{\partial u_1}{\partial x} + \gamma\frac{\partial P_1}{\partial x} + An_0\gamma\frac{\partial n_1}{\partial x} + An_0^2u_0\gamma^3\frac{\partial u_1}{\partial x} = 0. \tag{C15c}$$

First-order correction:

$$\frac{\partial n_2}{\partial t_0} + \gamma^2 n_0u_0\frac{\partial u_2}{\partial t_0} + u_0\frac{\partial n_2}{\partial x} + n_0\gamma^2\frac{\partial u_2}{\partial x} = \mathrm{RHS}, \tag{C16a}$$

$$\gamma^2\frac{\partial \varepsilon_2}{\partial t_0} + \gamma^2u_0^2\frac{\partial P_2}{\partial t_0} + 2u_0(\varepsilon_0+P_0)\gamma^4\frac{\partial u_2}{\partial t_0} + \left(1+u_0^2\right)(\varepsilon_0+P_0)\gamma^4\frac{\partial u_2}{\partial x} + u_0\gamma^2\frac{\partial}{\partial x}(\varepsilon_2+P_2) + An_0u_0\gamma\frac{\partial n_2}{\partial x} = \mathrm{RHS}, \tag{C16b}$$

$$\gamma^3(\varepsilon_0+P_0)\frac{\partial u_2}{\partial t_0} + \gamma u_0\frac{\partial P_2}{\partial t_0} + u_0\gamma^3(\varepsilon_0+P_0)\frac{\partial u_2}{\partial x} + \gamma\frac{\partial P_2}{\partial x} + An_0\frac{\partial n_2}{\partial x} = \mathrm{RHS}. \tag{C16c}$$

Again, we have used the electrostatic coupling A according to Eq. (28). See Appendix D for the terms on the right-hand side.

3. Leading-order equations

Using $\varepsilon = Pd$ and combining equations like

$$\left(\frac{\partial}{\partial t_0} + u_0\frac{\partial}{\partial x}\right)\left\{Adn_0\gamma^2\frac{\partial}{\partial x}[\text{Eq. (C15a)}] + \left(u_0\frac{\partial}{\partial t_0} + \frac{\partial}{\partial x}\right)[\text{Eq. (C15b)}] - \gamma\left(\left(d+u_0^2\right)\frac{\partial}{\partial t_0} + u_0(d+1)\frac{\partial}{\partial x}\right)[\text{Eq. (C15c)}]\right\}$$

gives

$$0 = \gamma^2\left(\frac{\partial}{\partial t_0} + u_0\frac{\partial}{\partial x}\right)\left\{\gamma^2(d+1)P_0\left(u_0^2-d\right)\frac{\partial^2 u_1}{\partial t_0^2} - 2\gamma^2(d+1)P_0u_0(d-1)\frac{\partial^2 u_1}{\partial t_0\partial x} + \left[Adn_0^2 + \gamma^2(d+1)P_0\left(1-du_0^2\right)\right]\frac{\partial^2 u_1}{\partial x^2}\right\}. \tag{C17}$$

This wave equation has solutions $f(x+v_0t_0) + g(x-v_0t_0)$ with v_0 given by

$$v_0^{(\pm)} = -\frac{u_0(d-1)}{d-u_0^2} \pm \frac{\sqrt{d}}{\left(d-u_0^2\right)\gamma^2}\sqrt{1+\frac{An_0^2\gamma^2\left(d-u_0^2\right)}{P_0(d+1)}}. \tag{C18}$$

We will take the $(+)$ sign so that $v_0 = v_0^{(+)}$; the other can be recovered by taking $u_0 \to -u_0$ and $v_0 \to -v_0$. Further, we restrict to unidirectional solutions $u_1(x,t_0,t_1) = f(x \pm v_0t_0, t_1)$ for a definite choice of $\pm$; here, we choose $(+)$ as well—the other propagation direction can be recovered by taking $v_0 \to -v_0$.

For stationary perturbations ($v_0 = 0$), we can solve for u_0:

$$u_0 = \pm\sqrt{\frac{(1/d) + \left[An_0^2/P_0(d+1)\right]}{1+\left[An_0^2/P_0(d+1)\right]}}. \tag{C19}$$

For reference, the velocity of propagation in the absence of a background flow ($u_0 = 0$) is

$$v_0 = \pm\frac{1}{\sqrt{d}}\sqrt{1+\frac{Adn_0^2}{(d+1)P_0}}. \tag{C20}$$

In general, n_1, u_1, and P_1 have traveling-wave solutions; neglecting solutions of the form $f(x-u_0t_0,t_1)$ that are simply advected by the background current, we find solutions given by

$$n_1(x,t_0,t_1) = n_1(x+v_0t_0,t_1) + F_1(t_1), \tag{C21a}$$

$$u_1(x,t_0,t_1) = -\frac{(u_0+v_0)}{n_0\gamma^2(1+u_0v_0)}n_1(x+v_0t_0,t_1) + F_2(t_1), \tag{C21b}$$

$$\frac{P_1(x,t_0,t_1)}{P_0} = \frac{d+1}{d}\frac{n_1(x+v_0t_0,t_1)}{n_0} + F_3(t_1). \tag{C21b}$$

Here, we have arbitrary functions $F_1(t_1)$, $F_2(t_2)$, and $F_3(t_2)$; by imposing boundary conditions $n_1 = 0$ at $x = \pm\infty$, we set $F_1 = 0$. We will allow $U_1(t_2) := F_2(t_2)$ to remain arbitrary; this uniform background current can be superimposed on the soliton solution as in Sec. IV if desired [59]. In the Dirac regime, we can impose $P_1 = 0$ at $x = \pm\infty$ to set $F_3 = 0$; however, for the Fermi regime, requiring that $T_0(x,t) = T_0$ independent of (x,t) restricts the relationship between P_1 and n_1. Hence, we will write F_3 as

$$F_3(t_1) = \delta_{m,-1}\frac{1}{d}\frac{\mathcal{C}_1}{\mathcal{C}_0}\left(\frac{T_0}{\mu_0}\right)^2. \tag{C22}$$

4. First-order corrections

Now considering the first-order corrections, preventing secular growth of the higher-order terms (i.e., n_2, u_2, etc.) requires imposing a compatibility condition on the lower-order terms (i.e., n_1, u_1, etc.). We can manipulate the system as

$$\left(\frac{\partial}{\partial t_0} + u_0\frac{\partial}{\partial x}\right)\left\{Adn_0\gamma^2\frac{\partial}{\partial x}[\text{Eq. (C16a)}] + \left(u_0\frac{\partial}{\partial t_0} + \frac{\partial}{\partial x}\right)[\text{Eq. (C16b)}] - \gamma\left[\left(d+u_0^2\right)\frac{\partial}{\partial t_0} + u_0(d+1)\frac{\partial}{\partial x}\right][\text{Eq. (C16c)}]\right\}$$
$$+ \delta_{m,-1}\gamma\frac{1}{2}\frac{\mathcal{C}_0}{\mathcal{C}_1}\frac{\sigma_Q(d+1)}{n_0}\frac{\mu_0^3}{T_0^2}\left(\frac{\partial}{\partial x} + u_0\frac{\partial}{\partial t_0}\right)^2\left(-\left(\frac{\partial}{\partial x}+u_0\frac{\partial}{\partial t_0}\right)[\text{Eq. (C16b)}] + \gamma\left[\left(d+u_0^2\right)\frac{\partial}{\partial t_0}+u_0(d+1)\frac{\partial}{\partial x}\right][\text{Eq. (C16c)}]\right.$$
$$\left. + \frac{Adn_0^2}{P_0(d+1)}\frac{\partial}{\partial x}\{\gamma u_0[\text{Eq. (C16c)}] - [\text{Eq. (C16b)}]\}\right)$$

to obtain

$$\gamma^4 P_0(d+1)\big(d-u_0^2\big)\left[\left(\frac{\partial}{\partial t_0}+u_0\frac{\partial}{\partial x}\right)-\delta_{m,1}\gamma\frac{1}{2}\frac{\mathcal{C}_0}{\mathcal{C}_1}\frac{\sigma_Q(d+1)}{n_0}\frac{\mu_0^3}{T_0^2}\left(\frac{\partial}{\partial x}+u_0\frac{\partial}{\partial t_0}\right)^2\right]\left(v_0^{(+)}\frac{\partial}{\partial x}-\frac{\partial}{\partial t_0}\right)\left(v_0^{(-)}\frac{\partial}{\partial x}-\frac{\partial}{\partial t_0}\right)u_2=\text{LOT}, \tag{C23}$$

where LOT represents lower-order terms (i.e., n_1, u_1, etc.).

It is instructive here to change variables to $\chi_0^{(\pm)}=x+v_0^{(\pm)}t_0$. Then, the equation becomes

$$\gamma^4 P_0(d+1)\big(d-u_0^2\big)(v_0^{(+)}-v_0^{(-)})^2\left\{\left[\sum_{\pm}(u_0+v_0^{(\pm)})\frac{\partial}{\partial\chi_0^{(\pm)}}\right]-\delta_{m,-1}\gamma\frac{3\sigma_Q}{\pi^2 n_0 d}\frac{\mu_0^3}{T_0^2}\left[\sum_{\pm}(1+u_0v_0^{(\pm)})\frac{\partial}{\partial\chi_0^{(\pm)}}\right]^2\right\}$$
$$\times\frac{\partial}{\partial\chi_0^{(-)}}\frac{\partial}{\partial\chi_0^{(+)}}u_2=\text{LOT}. \tag{C24}$$

This is where we encounter an apparent problem. Upon inserting our solutions for the lower-order terms, we find the right-hand side depends on products and derivatives of $f(\chi_0^{(+)})$. This implies that the LOT is solely a function of $\chi_0^{(+)}$.

However, we see that functions of the form $f(\chi^{(+)})$ are also solutions to the homogeneous equation in Eq. (C23) due to the presence of the $\partial_{\chi_0^{(-)}}$ operator. So, products and derivatives of $f(\chi_0^{(+)})$ appear as inhomogeneous forcing terms that give rise to secular terms. For instance, terms proportional to $f^{(4)}(\chi_0^{(+)})$ give rise to solutions of the form $\chi_0^{(-)}f^{(3)}(\chi_0^{(+)})$. This grows unbounded in $\chi_0^{(-)}$—and hence, in time t. This will eventually cause $|u_2|>|u_1|$, invalidating the perturbation expansion. Thus, unless LOT vanishes identically, it will give rise to $\chi_0^{(\pm)}$-secular terms in u_2—i.e., solutions growing unbounded in t_0 or x.

Hence, we require the right-hand side to vanish and we are left with the desired compatibility equation:

$$0=(u_0+v_0)\frac{\partial^2}{\partial\chi_0^{(+)^2}}(\text{KdVB}[n_1])-\delta_{m,-1}\gamma\frac{1}{2}\frac{\mathcal{C}_0}{\mathcal{C}_1}\frac{\sigma_Q(d+1)(1+u_0v_0)^2}{n_0}\frac{\mu_0^3}{T_0^2}\frac{\partial^3}{\partial\chi_0^{(+)^2}}(\text{KdVB}[n_1])\Big|_{\sigma_Q=0}. \tag{C25}$$

Here, (KdVB$[n_1]$) represents the Korteweg–de Vries–Burgers equation, discussed earlier, acting on n_1:

$$\mathcal{A}'\frac{\partial n_1}{\partial t_1}+\mathcal{F}'\frac{\partial n_1}{\partial\chi_0^{(+)}}+\mathcal{B}'n_1\frac{\partial n_1}{\partial\chi_0^{(+)}}+\mathcal{C}'\frac{\partial^3 n_1}{\chi_0^{(+)^3}}-\mathcal{G}'\frac{\partial^2 n_1}{\chi_0^{(+)^2}}n_1=0; \tag{C26}$$

see Appendix F for the functional form of the coefficients. Likewise, (KdVB$[n_1]|_{\sigma_Q=0}$) represents the Korteweg–de Vries–Burgers equation without σ_Q terms.

It is interesting to note the similarities and differences between the adiabatic KdV-Burgers coefficients (Appendix F) and the isothermal coefficients (Appendix E). For most of the coefficients ($\mathcal{A}'$, $\mathcal{B}'$, and $\mathcal{C}'$), the adiabatic coefficients are identical to the isothermal Fermi ($m=-1$) coefficients. The $(1+u_0v_0)\mathcal{C}_1/\mathcal{C}_0$ term in $\mathcal{F}'$ differs slightly between the adiabatic Fermi case [coefficient $(d+1)/d^2$] and the isothermal Fermi case [coefficient $(d-1)/d^2$]; the adiabatic Dirac case is completely absent ($\delta_{m,-1}$) compared to the isothermal Dirac case. Interestingly, the adiabatic η and ζ terms in $\mathcal{G}'$ match the isothermal Fermi terms, while the adiabatic σ_Q term matches the isothermal Dirac one.

5. Solving the compatibility equation

In the Fermi regime ($m=-1$), the compatibility equation (C25) no longer has the simple, decaying soliton solution derived in Sec. IV F. This can certainly be solved numerically. Additionally, we can generate an approximate solution if we assume that $O(\sigma_Q)\ll 1$ (but $\gg\epsilon$ to prevent them from falling to the next order in our perturbation expansion) and use the same trick as we did in Sec. IV F. Namely, we factor out a small parameter $\delta\sim O(\sigma_Q)$ from $\sigma_Q=\delta\tilde{\sigma}_Q$. Then, $O(\tilde{\sigma}_Q)=1$, and we can expand in factors of δ.

Then, another short multiple scales expansion for n_1 can be done in $\delta=O(\mathcal{G}/\mathcal{A})$. To be consistent with our original perturbation series, we require that $\epsilon\ll\delta\ll 1$. As usual, we expand n_1 as $n_1=n_1^{(0)}+\delta n_1^{(1)}$ and $\partial_{t_1}=\partial_{\tau_0}+\delta\partial_{\tau_1}$. Then, to leading order, we have

$$(u_0+v_0)\partial^2_{\chi_0^{(+)}}\big(\text{KdVB}\big[n_1^{(0)}\big]\big)\big|_{\tilde{\sigma}_Q=0}=0. \tag{C27}$$

This is satisfied by the KdVB equation,

$$\mathcal{L}_0 n_1^{(0)}:=\mathcal{A}'\partial_{\tau_0}n_1^{(0)}+\mathcal{F}'\partial_{\chi_0^{(+)}}n_1^{(0)}+\frac{\mathcal{B}'}{2}\partial_{\chi_0^{(+)}}\big(n_1^{(0)}\big)^2+\mathcal{C}'\partial^3_{\chi_0^{(+)}}n_1^{(0)}-\mathcal{G}'\Big|_{\tilde{\sigma}_Q=0}\partial^2_{\chi_0^{(+)}}n_1^{(0)}=0. \tag{C28}$$

Now, we further assume that η and ζ are small; specifically, we assume $O(\eta) \ll 1, \epsilon \ll O(\delta) \ll O(\zeta)$. Then, the solution was found in Sec. IV F upon replacing $\mathcal{G}'$ with $\mathcal{G}'|_{\tilde{\sigma}_Q=0}$:

$$n_1^{(0)}(\chi_0^{(+)}, \tau_0) = c_1(\tau_0)\mathrm{sgn}(\mathcal{B}'\mathcal{C}')\,\mathrm{sech}^2\left(\sqrt{\frac{c_1|\mathcal{B}'|}{12|\mathcal{C}'|}}\left[\chi_0^{(+)} - \left(\frac{c_1|\mathcal{B}'|}{3|\mathcal{A}'|}\mathrm{sgn}(\mathcal{A}'\mathcal{C}') + \frac{\mathcal{F}'}{\mathcal{A}'}\right)\tau_0\right]\right), \tag{C29}$$

where

$$c_1(\tau_0) = \frac{c_1(0)}{1 + \tau_0/\tau_d^{(0)}} \tag{C30}$$

with

$$\tau_d^{(0)} = \frac{45\mathcal{A}'|\mathcal{C}'|}{4c_1(0)|\mathcal{B}'|\mathcal{G}'|_{\tilde{\sigma}_Q=0}}. \tag{C31}$$

As mentioned above, we have assumed $O(\delta) \ll O(\mathcal{G}'/\mathcal{A}'|_{\tilde{\sigma}_Q=0}) \ll 1$, so $1/\tau_d^{(0)} \ll 1$.

At the next order in δ, we must allow the constant $c_1(0)$ to become time-dependent on a slow timescale $c_1(0) = c_1(0, \tau_1)$. Now, our equation is

$$\begin{aligned}
&(u_0 + v_0)\partial^2_{\chi_0^{(+)}}\left[\mathcal{A}'\partial_{\tau_0}n_1^{(1)} + \mathcal{F}'\partial_{\chi_0^{(+)}}n_1^{(1)} + \mathcal{B}'\partial_{\chi_0^{(+)}}\left(n_1^{(0)}n_1^{(1)}\right) + \mathcal{C}'\partial^3_{\chi_0^{(+)}}n_1^{(1)}\right] \\
&= (u_0 + v_0)\partial^2_{\chi_0^{(+)}}\left(-\partial_{t_1}\mathcal{A}'n_1^{(0)} + \partial^4_{\chi_0^{(+)}}\mathcal{G}'n_1^{(0)}\right) - \delta_{m,-1}\gamma\frac{1}{2}\frac{\mathcal{C}_0}{\mathcal{C}_1}\frac{\sigma_Q(d+1)(1+u_0v_0)^2}{n_0}\frac{\mu_0^3}{T_0^2}\partial\chi_0^{(+)^3}\left(\mathrm{KdVB}\left[n_1^{(0)}\right]\right)\Big|_{\tilde{\sigma}_Q=0} \\
&= (u_0 + v_0)\partial^2_{\chi_0^{(+)}}\left(-\partial_{t_1}\mathcal{A}'n_1^{(0)} + \partial^2_{\chi_0^{(+)}}\mathcal{G}'n_1^{(0)}\right).
\end{aligned} \tag{C32}$$

In the last line, we used the fact that $n_1^{(0)}$ satisfies the $\mathrm{KdVB}|_{\tilde{\sigma}_Q=0}$ equation to simplify the right-hand side. Integrating twice and dropping constants of integration (we want $n_1^{(0)} = n_1^{(1)} = 0$ to be a solution) gives

$$\begin{aligned}
\mathcal{L}_1 n_1^{(1)} &:= \mathcal{A}'\partial_{\tau_0}n_1^{(1)} + \mathcal{F}'\partial_{\chi_0^{(+)}}n_1^{(1)} + \mathcal{B}'\partial_{\chi_0^{(+)}}\left(n_1^{(0)}n_1^{(1)}\right) + \mathcal{C}'\partial^3_{\chi_0^{(+)}}n_1^{(1)} \\
&= -\partial_{t_1}\mathcal{A}'n_1^{(0)} + \partial^2_{\chi_0^{(+)}}\mathcal{G}'n_1^{(0)}.
\end{aligned} \tag{C33}$$

As before, we note that $\mathcal{L}_0$ and $-\mathcal{L}_1$ are adjoint:

$$\int d\chi_0^{(+)}\left(n_1^{(1)}\mathcal{L}_0 n_1^{(0)} + n_1^{(0)}\mathcal{L}_1 n_1^{(1)}\right) = 0. \tag{C34}$$

Thus, we get the compatibility condition

$$(u_0 + v_0)\int n_1^{(0)}\left(\mathcal{A}'\partial_{\tau_1}n_1^{(0)} - \mathcal{G}'\partial_x^2 n_1^{(0)}d\chi_0^{(+)}\right) = 0, \tag{C35}$$

which yields the equation

$$\partial_{\tau_1}c_1(0, \tau_1) = -\frac{c_1(0, \tau_1)^2|\mathcal{B}'|\tilde{\mathcal{G}}'}{|\mathcal{C}'|\mathcal{A}'}\frac{4}{45}. \tag{C36}$$

Then, solving this equation and converting back to time t_1 gives

$$c_1(0, t_1) = \frac{c_1(0, 0)}{1 + t_1/t_d^{(1)}} \tag{C37}$$

with

$$t_d^{(1)} = \frac{45\mathcal{A}'|\mathcal{C}'|}{4c_1(0, 0)|\mathcal{B}'|\mathcal{G}'}, \tag{C38}$$

with $c_1(0, 0)$ the initial value of the parameter $c_1(t_0, t_1)$. Combined with the result for $c_1(t_0, t_1)$ [Eqs. (C30) and (C31)],

$$c_1(t_0, t_1) = \frac{c_1(0, t_1)}{1 + t_0/t_d^{(0)}} \tag{C39}$$

with

$$t_d^{(0)} = \frac{45\mathcal{A}'|\mathcal{C}'|}{4c_1(0, t_1)|\mathcal{B}'|\mathcal{G}'|_{\sigma_Q=0}}, \tag{C40}$$

we now have a complete solution.

APPENDIX D: FULL EQUATIONS

All quantities are expressed in normalized, nondimensional form according to the procedures laid out in Sec. III and Appendix B. The energy conservation equations [Eqs. (D1b) and (D2b)] are only used for the adiabatic setup.

Leading order:

$$\frac{\partial n_1}{\partial t_0}+\gamma^2 n_0 u_0\frac{\partial u_1}{\partial t_0}+u_0\frac{\partial n_1}{\partial x}+n_0\gamma^2\frac{\partial u_1}{\partial x}=0, \tag{D1a}$$

$$\gamma^2\frac{\partial \varepsilon_1}{\partial t_0}+\gamma^2 u_0^2\frac{\partial P_1}{\partial t_0}+2u_0(\varepsilon_0+P_0)\gamma^4\frac{\partial u_1}{\partial t_0}+\left(1+u_0^2\right)(\varepsilon_0+P_0)\gamma^4\frac{\partial u_1}{\partial x}+u_0\gamma^2\frac{\partial}{\partial x}(\varepsilon_1+P_1)+An_0u_0\gamma^2\frac{\partial n_1}{\partial x}+An_0^2u_0^2\gamma^4\frac{\partial u_1}{\partial x}=0, \tag{D1b}$$

$$\gamma^3(\varepsilon_0+P_0)\frac{\partial u_1}{\partial t_0}+\gamma u_0\frac{\partial P_1}{\partial t_0}+u_0\gamma^3(\varepsilon_0+P_0)\frac{\partial u_1}{\partial x}+\gamma\frac{\partial P_1}{\partial x}+An_0\gamma\frac{\partial n_1}{\partial x}+An_0^2u_0\gamma^3\frac{\partial u_1}{\partial x}=0. \tag{D1c}$$

First-order corrections:

$$\begin{aligned}
&\frac{\partial n_2}{\partial t_0}+\gamma^2 n_0u_0\frac{\partial u_2}{\partial t_0}+u_0\frac{\partial n_2}{\partial x}+n_0\gamma^2\frac{\partial u_2}{\partial x}\\
&\quad=-\frac{\partial n_1}{\partial t_1}-n_0u_0\gamma^2\frac{\partial u_1}{\partial t_1}-u_0u_1\gamma^2\frac{\partial n_1}{\partial t_0}-\gamma^2\left[\gamma^2\left(1+2u_0^2\right)n_0u_1+u_0n_1\right]\frac{\partial u_1}{\partial t_0}\\
&\qquad-\gamma^2\left[u_0\gamma^2\left(2+u_0^2\right)n_0u_1+n_1+n_0u_0u_1\right]\frac{\partial u_1}{\partial x}-\gamma^2u_1\frac{\partial n_1}{\partial x}\\
&\qquad+\gamma u_0A\sigma_Q\frac{\partial^2 n_1}{\partial t_0\partial x}+\gamma A\sigma_Q\frac{\partial^2 n_1}{\partial x^2}+\gamma^3u_0A\sigma_Qn_0\left(\frac{\partial^2 u_1}{\partial x^2}+u_0\frac{\partial^2 u_1}{\partial t_0\partial x}\right)\\
&\qquad+\Theta(-m)\gamma\sigma_Q\left[\left(u_0^2\frac{\partial^2\mu_1}{\partial t_0^2}+2u_0\frac{\partial^2\mu_1}{\partial t_0\partial x}+\frac{\partial^2\mu_1}{\partial x^2}\right)-\frac{\mu_0}{T_0}\left(u_0^2\frac{\partial^2 T_1}{\partial t_0^2}+2u_0\frac{\partial^2 T_1}{\partial t_0\partial x}+\frac{\partial^2 T_1}{\partial x^2}\right)\right],
\end{aligned} \tag{D2a}$$

$$\begin{aligned}
&\gamma^2\frac{\partial \varepsilon_2}{\partial t_0}+\gamma^2u_0^2\frac{\partial P_2}{\partial t_0}+2u_0(\varepsilon_0+P_0)\gamma^4\frac{\partial u_2}{\partial t_0}+\left(1+u_0^2\right)(\varepsilon_0+P_0)\gamma^4\frac{\partial u_2}{\partial x}+u_0\gamma^2\frac{\partial}{\partial x}(\varepsilon_2+P_2)+An_0u_0\gamma^2\frac{\partial n_2}{\partial x}+An_0^2u_0^2\gamma^4\frac{\partial u_2}{\partial x}\\
&\quad=-2(\varepsilon_0+P_0)u_0\gamma^4\frac{\partial u_1}{\partial t_1}-\gamma^2\frac{\partial \varepsilon_1}{\partial t_1}-\gamma^2u_0^2\frac{\partial P_1}{\partial t_1}-2(\varepsilon_0+P_0)\gamma^6\left(1+3u_0^2\right)u_1\frac{\partial u_1}{\partial t_0}-2(\varepsilon_1+P_1)\gamma^4u_0\frac{\partial u_1}{\partial t_0}\\
&\qquad-2u_0u_1\gamma^4\frac{\partial}{\partial t_0}(\varepsilon_1+P_1)-2\left(3+u_0^2\right)u_0u_1\gamma^6(\varepsilon_0+P_0)\frac{\partial u_1}{\partial x}-\gamma^4\left(1+u_0^2\right)(\varepsilon_1+P_1)\frac{\partial u_1}{\partial x}-\left(1+u_0^2\right)u_1\gamma^4\frac{\partial}{\partial x}(\varepsilon_1+P_1)\\
&\qquad+\gamma^5u_0\left[\zeta+2\eta\left(1-\frac{1}{d}\right)\left(u_0^2\frac{\partial^2 u_1}{\partial t_0^2}+2u_0\frac{\partial^2 u_1}{\partial t_0\partial x}+\frac{\partial^2 u_1}{\partial x}\right)\right]\\
&\qquad-An_0u_1\gamma^4\frac{\partial n_1}{\partial x}-Au_0n_1\gamma^2\frac{\partial n_1}{\partial x}-An_0u_0\gamma^2\frac{d_1d_2}{3}\frac{\partial^3 n_1}{\partial x^3}-2An_0^2u_0\left(1+u_0^2\right)u_1\gamma^6\frac{\partial u_1}{\partial x}\\
&\qquad-2An_0u_0^2n_1\gamma^4\frac{\partial u_1}{\partial x}-An_0^2u_0^2\gamma^4\frac{d_1d_2}{3}\frac{\partial^3 u_1}{\partial x}-An_0u_0^2u_1\gamma^4\frac{\partial n_1}{\partial x},
\end{aligned} \tag{D2b}$$

$$\begin{aligned}
&\gamma^3(\varepsilon_0+P_0)\frac{\partial u_2}{\partial t_0}+\gamma u_0\frac{\partial P_2}{\partial t_0}+u_0\gamma^3(\varepsilon_0+P_0)\frac{\partial u_2}{\partial x}+\gamma\frac{\partial P_2}{\partial x}+An_0\gamma\frac{\partial n_2}{\partial x}+An_0^2u_0\gamma^3\frac{\partial u_2}{\partial x}\\
&\quad=-(\varepsilon_0+P_0)\gamma^3\frac{\partial u_1}{\partial t_1}-u_0\gamma\frac{\partial P_1}{\partial t_1}-\gamma^3[2u_0u_1\gamma^2(\varepsilon_0+P_0)+(\varepsilon_1+P_1)]\frac{\partial u_1}{\partial t_0}-u_1\gamma\frac{\partial P_1}{\partial t_0}\\
&\qquad-\gamma^3\left[u_0(\varepsilon_1+P_1)+\left(1+u_0^2\right)u_1\gamma^2(\varepsilon_0+P_0)\right]\frac{\partial u_1}{\partial x}-An_1\gamma\frac{\partial n_1}{\partial x}-An_0\gamma\frac{d_1d_2}{3}\frac{\partial^3 n_1}{\partial x^3}\\
&\qquad-An_0^2\left(1+u_0^2\right)u_1\gamma^5\frac{\partial u_1}{\partial x}-An_0^2u_0\gamma^3\frac{d_1d_2}{3}\frac{\partial^3 u_1}{\partial x^3}-2An_0u_0n_1\gamma^3\frac{\partial u_1}{\partial x}\\
&\qquad+\gamma^4\left[\zeta+2\eta\left(1-\frac{1}{d}\right)\right]\left(u_0^2\frac{\partial^3 u_1}{\partial t_0}+2u_0\frac{\partial^2 u_1}{\partial t_0\partial x}+\frac{\partial^2 u_1}{\partial x}\right).
\end{aligned} \tag{D2c}$$

APPENDIX E: ISOTHERMAL KdV-BURGERS

All quantities are expressed in dimensional form; to get the dimensionless expressions, simply set $v_F = \hbar = l_{\rm ref} = k_B = e = 1$ and remove all factors of ϵ. See Appendix A for the values of $\mathcal{C}_0$ and $\mathcal{C}_1$ and Appendix B for the O expressions. The KdV-Burgers equation is given by

$$\frac{\mathcal{A}'}{v_F}\frac{\partial n_1}{\partial t_1} + \mathcal{F}'\frac{\partial n_1}{\partial x} + \mathcal{B}'\frac{l_{\rm ref}^d}{O\left(n l_{\rm ref}^d\right)} n_1 \frac{\partial n_1}{\partial x} + \mathcal{C}'\frac{l_{\rm ref}^2}{O(\partial_x l_{\rm ref})^2}\frac{\partial^3 n_1}{\partial x^3} = \mathcal{G}'\frac{l_{\rm ref}}{O(\partial_x l_{\rm ref})}\frac{\partial^2 n_1}{\partial x^2}, \tag{E1}$$

with

$$\mathcal{A}' = 2\gamma^2 \frac{u_0+v_0}{v_F^2+u_0v_0}\frac{P_0 l_{\rm ref} d}{n_0\hbar v_F^3}\left\{v_0\left[v_F^2(d+1)-u_0^2K_0\right]+u_0v_F^2(d+1-K_0)\right\}, \tag{E2}$$

$$\mathcal{B}' = -\gamma^2\frac{u_0+v_0}{v_F^2+u_0v_0}\frac{P_0 l_{\rm ref}^{1-d}}{n_0^2 d\hbar v_F^4}\left\{d^2v_F^2(u_0+v_0)^2[4(d+1)-K_0(d+3)]+\left(v_F^2+u_0v_0\right)^2[(d+1)\Theta(-m)-K_0d^2]\right\}O\left(n l_{\rm ref}^d\right), \tag{E3}$$

$$\mathcal{C}' = -\frac{n_0}{\epsilon l_{\rm ref}\hbar}Ad\frac{d_1d_2}{3}\frac{u_0+v_0}{v_F^2+u_0v_0}O(\partial_x l_{\rm ref})^2, \tag{E4}$$

$$\begin{aligned}\mathcal{F}' = \gamma^2\frac{P_0 l_{\rm ref} d}{\epsilon n_0\hbar v_F^4}\frac{u_0+v_0}{v_F^2+u_0v_0}\Bigg\{&2U_1\gamma^2(d+1-K_0)(u_0+v_0)\left(v_F^2+u_0v_0\right)\\ &+\frac{\mathcal{C}_1}{\mathcal{C}_0}\left(\frac{\mu_0}{k_BT_0}\right)^{2m}\left[v_F^2(u_0+v_0)^2(d+1)\left(\frac{1}{d}\delta_{m,-1}+\delta_{m,1}\right)-\left(v_F^2+u_0v_0\right)^2\left(\frac{d-1}{d^2}\delta_{m,-1}+2\delta_{m,1}\right)\right]\Bigg\},\end{aligned} \tag{E5}$$

$$\begin{aligned}\mathcal{G}' = \frac{\gamma^3\left(v_F^2+u_0v_0\right)}{\epsilon n_0\hbar v_F^{10}}\Bigg\{&\frac{\sigma_Q}{e^2}\gamma^2\left(\frac{P_0}{n_0}\right)^2(u_0+v_0)\left(v_F^2+u_0v_0\right)(d+1)\left[v_0\left[v_F^2(d+1)-u_0^2K_0\right]+u_0v_F^2(d+1-K_0)\right]\\ &\times\left[\frac{d(u_0+v_0)^2}{\left(v_F^2+u_0v_0\right)^2}+\underbrace{\Theta(-m)-K_0\frac{d}{d+1}}_{=0}\right]+v_F^6d(u_0+v_0)^2\left[\zeta+2\eta\left(1-\frac{1}{d}\right)\right]\Bigg\}O(\partial_x l_{\rm ref}),\end{aligned} \tag{E6}$$

and

$$v_0^{(\pm)} = v_F^2\frac{-u_0(d+1-K_0)\pm\frac{1}{\gamma}\sqrt{\left[K_0(d+1)v_F^2\right]/\gamma^2+\left(An_0^2/P_0\right)\left[v_F^2(d+1)-u_0^2K_0\right]}}{v_F^2(d+1)-u_0^2K_0}. \tag{E7}$$

If we impose $v_0 = 0$, then the coefficients take the form given in Eq. (60). If instead we impose $u_0 = U_1 = 0$, they take the form

$$\mathcal{A}' = 2\frac{P_0(d+1)v_0^2 l_{\rm ref} d}{n_0\hbar v_F^3}, \tag{E8}$$

$$\mathcal{B}' = -v_0\frac{P_0 l_{\rm ref}^{1-d}}{n_0^2 d\hbar v_F^4}\left\{d^2v_0^2[4(d+1)-K_0(d+3)]+v_F^2\left[(d+1)\Theta(-m)-K_0d^2\right]\right\}O\left(n l_{\rm ref}^d\right), \tag{E9}$$

$$\mathcal{C}' = -\frac{n_0}{\epsilon l_{\rm ref}\hbar v_F^2}Ad\frac{d_1d_2}{3}v_0O(\partial_x l_{\rm ref})^2, \tag{E10}$$

$$\mathcal{F}' = \frac{P_0 l_{\rm ref} d}{\epsilon n_0\hbar v_F^4}v_0\frac{\mathcal{C}_1}{\mathcal{C}_0}\left(\frac{\mu_0}{k_BT_0}\right)^{2m}\left[v_0^2(d+1)\left(\frac{1}{d}\delta_{m,-1}+\delta_{m,1}\right)-v_F^2\left(\frac{d-1}{d^2}\delta_{m,-1}+2\delta_{m,1}\right)\right], \tag{E11}$$

$$\mathcal{G}' = \frac{1}{\epsilon n_0\hbar v_F^4}\left\{\frac{\sigma_Q}{e^2}\left(\frac{P_0}{n_0}\right)^2v_0^2(d+1)^2\left[\frac{v_0^2d}{v_F^2}+\underbrace{\Theta(-m)-K_0\frac{d}{d+1}}_{=0}\right]+v_0^2v_F^2d\left[\zeta+2\eta\left(1-\frac{1}{d}\right)\right]\right\}O(\partial_x l_{\rm ref}), \tag{E12}$$

with

$$v_0 = \pm\frac{v_F}{\sqrt{d+1}}\sqrt{K_0+\frac{An_0^2}{P_0}}. \tag{E13}$$

APPENDIX F: ADIABATIC KdV-BURGERS

All quantities are expressed in dimensional form; to get the dimensionless expressions, simply set $v_F = \hbar = l_{\rm ref} = k_B = e = 1$ and remove all factors of ϵ. See Appendix A for the values of $\mathcal{C}_0$ and $\mathcal{C}_1$ and Appendix B for the O expressions. The KdV-Burgers equation is given by

$$\frac{\mathcal{A}'}{v_F}\frac{\partial n_1}{\partial t_1} + \mathcal{F}'\frac{\partial n_1}{\partial x} + \mathcal{B}'\frac{l_{\rm ref}^d}{O(n) l_{\rm ref}^d} n_1 \frac{\partial n_1}{\partial x} + \mathcal{C}'\frac{l_{\rm ref}^2}{O(\partial_x l_{\rm ref})^2}\frac{\partial^3 n_1}{\partial x^3} = \mathcal{G}'\frac{l_{\rm ref}}{O(\partial_x l_{\rm ref})}\frac{\partial^2 n_1}{\partial x^2}, \tag{F1}$$

with

$$\mathcal{A}' = 2\gamma^2 \frac{u_0+v_0}{v_F^2+u_0v_0}\frac{P_0(d+1)l_{\rm ref}}{n_0\hbar v_F^3}\left[v_0\left(v_F^2 d - u_0^2\right) + u_0 v_F^2(d-1)\right], \tag{F2}$$

$$\mathcal{B}' = -\gamma^2 \frac{u_0+v_0}{v_F^2+u_0v_0}\frac{P_0(d+1)l_{\rm ref}^{1-d}}{n_0^2\hbar v_F^4}\frac{d-1}{d}\left[3dv_F^2(u_0+v_0)^2 - \left(v_F^2+u_0v_0\right)^2\right]O\left(n l_{\rm ref}^d\right), \tag{F3}$$

$$\mathcal{C}' = -\frac{n_0}{\epsilon l_{\rm ref}\hbar} A d \frac{d_1 d_2}{3}\frac{u_0+v_0}{v_F^2+u_0v_0} O(\partial_x l_{\rm ref})^2, \tag{F4}$$

$$\mathcal{F}' = \gamma^2 \frac{P_0(d+1)l_{\rm ref}}{\epsilon n_0\hbar v_F^4}\frac{u_0+v_0}{v_F^2+u_0v_0}\left\{2U_1\gamma^2(d-1)(u_0+v_0)\left(v_F^2+u_0v_0\right) + \delta_{m,-1}\frac{1}{d}\frac{\mathcal{C}_1}{\mathcal{C}_0}\left(\frac{k_B T_0}{\mu_0}\right)^2\left[dv_F^2(u_0+v_0)^2 - \left(v_F^2+u_0v_0\right)^2\right]\right\}, \tag{F5}$$

$$\mathcal{G}' = \frac{d\gamma\left(v_F^2+u_0v_0\right)}{\epsilon n_0\hbar v_F^4}\left\{\frac{\sigma_Q}{e^2}\frac{A^2 n_0^2 v_F^2}{v_F^2+u_0v_0} + \gamma^2(u_0+v_0)^2\left[\zeta + 2\eta\left(1-\frac{1}{d}\right)\right]\right\} O(\partial_x l_{\rm ref}), \tag{F6}$$

and

$$v_0^{(\pm)} = -\frac{u_0 v_F^2(d-1)}{v_F^2 d - u_0^2} \pm \frac{v_F^2\sqrt{d}}{\left(v_F^2 d - u_0^2\right)\gamma^2}\sqrt{v_F^2 + \frac{A n_0^2\gamma^2\left(v_F^2 d - u_0^2\right)}{P_0(d+1)}}. \tag{F7}$$

If we impose $v_0 = 0$, then the coefficients take the form given in Eq. (60). If instead we impose $u_0 = U_1 = 0$, they take the form

$$\mathcal{A}' = 2\frac{P_0(d+1)v_0^2 l_{\rm ref} d}{n_0\hbar v_F^3}, \tag{F8}$$

$$\mathcal{B}' = -\frac{P_0(d+1)l_{\rm ref}^{1-d}}{n_0^2\hbar v_F^4}\frac{d-1}{d} v_0\left(3dv_0^2 - v_F^2\right) O\left(n l_{\rm ref}^d\right), \tag{F9}$$

$$\mathcal{C}' = -\frac{n_0}{\epsilon l_{\rm ref}\hbar v_F^2} A d \frac{d_1 d_2}{3} v_0 O(\partial_x l_{\rm ref})^2, \tag{F10}$$

$$\mathcal{F}' = \delta_{m,-1}\frac{A n_0 v_0 l_{\rm ref}}{\epsilon\hbar v_F^2}\frac{\mathcal{C}_1}{\mathcal{C}_0}\left(\frac{k_B T_0}{\mu_0}\right)^2, \tag{F11}$$

$$\mathcal{G}' = \frac{d}{\epsilon n_0\hbar v_F^2}\left\{\frac{\sigma_Q}{e^2}A^2 n_0^2 + v_0^2\left[\zeta + 2\eta\left(1-\frac{1}{d}\right)\right]\right\} O(\partial_x l_{\rm ref}), \tag{F12}$$

with

$$v_0 = \pm\frac{v_F}{\sqrt{d}}\sqrt{1 + \frac{A d n_0^2}{(d+1)P_0}}. \tag{F13}$$

[1] A. Lucas and K. C. Fong, Hydrodynamics of electrons in graphene, J. Phys.: Condens. Matter **30**, 053001 (2018).

[2] L. D. Landau and E. M. Lifshitz, *Fluid Mechanics*, Course of Theoretical Physics (Pergamon, London, 1959).

[3] L. D. Landau, The theory of a fermi liquid, J. Exp. Theor. Phys. **3**, 920 (1956).

[4] K. S. Novoselov, A. K. Geim, S. V. Morozov, D. Jiang, M. I. Katsnelson, I. V. Grigorieva, S. V. Dubonos, and A. A. Firsov, Two-dimensional gas of massless dirac fermions in graphene, Nature (London) **438**, 197 (2005).

[5] J. Crossno, J. K. Shi, K. Wang, X. Liu, A. Harzheim, A. Lucas, S. Sachdev, P. Kim, T. Taniguchi, K. Watanabe *et al.*, Observation of the dirac fluid and the breakdown of the wiedemann-franz law in graphene, Science **351**, 1058 (2016).

[6] I. Torre, A. Tomadin, A. K. Geim, and M. Polini, Nonlocal transport and the hydrodynamic shear viscosity in graphene, Phys. Rev. B **92**, 165433 (2015).

[7] A. Tomadin, G. Vignale, and M. Polini, Corbino Disk Viscometer for 2d Quantum Electron Liquids, Phys. Rev. Lett. **113**, 235901 (2014).

[8] L. Levitov and G. Falkovich, Electron viscosity, current vortices and negative nonlocal resistance in graphene, Nat. Phys. **12**, 672 (2016).

[9] M. Dyakonov and M. Shur, Shallow Water Analogy for a Ballistic Field Effect Transistor: New Mechanism of Plasma Wave Generation by dc Current, Phys. Rev. Lett. **71**, 2465 (1993).

[10] D. A. Bandurin, I. Torre, R. K. Kumar, M. B. Shalom, A. Tomadin, A. Principi, G. H. Auton, E. Khestanova, K. S. Novoselov, I. V. Grigorieva *et al.*, Negative local resistance caused by viscous electron backflow in graphene, Science **351**, 1055 (2016).

[11] R. K. Kumar, D. A. Bandurin, F. M. D. Pellegrino, Y. Cao, A. Principi, H. Guo, G. H. Auton, M. B. Shalom, L. A. Ponomarenko, G. Falkovich *et al.*, Superballistic flow of viscous electron fluid through graphene constrictions, Nat. Phys. **13**, 1182 (2017).

[12] A. Lucas and S. Das Sarma, Electronic sound modes and plasmons in hydrodynamic two-dimensional metals, Phys. Rev. B **97**, 115449 (2018).

[13] Z. Sun, D. N. Basov, and M. M. Fogler, Adiabatic Amplification of Plasmons and Demons in 2d Systems, Phys. Rev. Lett. **117**, 076805 (2016).

[14] M. Akbari-Moghanjoughi, Universal aspects of localized excitations in graphene, J. Appl. Phys. **114**, 073302 (2013).

[15] D. Svintsov, V. Vyurkov, V. Ryzhii, and T. Otsuji, Hydrodynamic electron transport and nonlinear waves in graphene, Phys. Rev. B **88**, 245444 (2013).

[16] Note that some of our variable definitions differ from those of Lucas and Fong [1] to better match usual conventions. The relevant changes (with the variables of Lucas and Fong [1] denoted by a subscript L) are $J^\mu = -eJ^\mu_{\rm L}$, $F^{\mu,\nu} = -F^{\mu\nu}_{\rm L}/e$, and $\sigma_Q = e^2\sigma_{Q,{\rm L}}$.

[17] Note that, as mentioned previously, $\delta \sim \partial$; the factor of $l_{\rm ee}$ is implicit in the definitions of the dissipative coefficients σ_Q, η, and ζ [1].

[18] R. N. Gurzhi, Minimum of resistance in impurity-free conductors, J. Exp. Theor. Phys. **17**, 521 (1963).

[19] D. A. Bandurin, A. V. Shytov, L. S. Levitov, R. K. Kumar, A. I. Berdyugin, M. B. Shalom, I. V. Grigorieva, A. K. Geim, and G. Falkovich, Fluidity onset in graphene, Nat. Commun. **9**, (2018).

[20] T. Stauber, N. M. R. Peres, and F. Guinea, Electronic transport in graphene: A semiclassical approach including midgap states, Phys. Rev. B **76**, 205423 (2007).

[21] The Stefan-Boltzmann law would give a power loss rate of $P_r = \sigma\epsilon[(T_0+T_1)^4 - T_0^4] \approx 4\sigma\epsilon T_0^3 T_1$, with $\sigma = 5.67 \times 10^{-8}\,{\rm W m^{-2} K^{-4}}$ and $\epsilon \leqslant 1$ graphene's emissivity. Using $\epsilon \approx 1\%$ [60], $T_0 = 60\,{\rm K}$, and $T_1 = 0.1\,T_0 = 6.0\,{\rm K}$, we find a power loss density of $P_r = 2.9 \times 10^{-7}\,{\rm kW\,cm^{-2}}$. As we will calculate in Sec. VII C, graphene has a specific heat of $c_s = 4.5 \times 10^{-9}\,{\rm J\,cm^{-2} K^{-1}}$. Therefore, the soliton's temperature will change at a rate of $P_r/c_s = 65\,{\rm K\,s^{-1}}$. Hence, it would take approximately $T_1 c_s/P_r = 93\,{\rm ms}$ for the system to thermalize with the environment via radiation.

[22] Z.-Y. Ong and E. Pop, Effect of substrate modes on thermal transport in supported graphene, Phys. Rev. B **84**, 075471 (2011).

[23] L. Chen, Z. Yan, and S. Kumar, Coupled electron-phonon transport and heat transfer pathways in graphene nanostructures, Carbon **123**, 525 (2017).

[24] P. Virtanen, Energy transport via multiphonon processes in graphene, Phys. Rev. B **89**, 245409 (2014).

[25] A. O. Govorov, V. M. Kovalev, and A. V. Chaplik, Solitons in semiconductor microstructures with a two-dimensional electron gas, JETP Lett. **70**, 488 (1999).

[26] After choosing $\hbar = v_F = k_B = e = 1$, all quantities will be expressed in various powers of length. If the parameters have been chosen correctly, there will exist a characteristic length Ξ shared by all quantities. It is most convenient to choose $l_{\rm ref} = \Xi$, though it is not strictly necessary—choosing $l_{\rm ref}$ otherwise will multiply all terms in each equation by the same factor of $l_{\rm ref}/\Xi$.

[27] As discussed in Appendix B 3, we could introduce three additional microscopic equations and eliminate η, ζ, and σ_Q/e^2 as independent quantities. However, we will refrain from doing so.

[28] L. Fritz, J. Schmalian, M. Müller, and S. Sachdev, Quantum critical transport in clean graphene, Phys. Rev. B **78**, 085416 (2008).

[29] C. C. Mei, M. Stiassnie, and D. K.-P. Yue, *Theory and Applications of Ocean Surface Waves: Nonlinear Aspects* (World Scientific, Singapore, 2005), Vol. 23.

[30] M. Akbari-Moghanjoughi, Higher-order nonlinear electron-acoustic solitary excitations in partially degenerate quantum electron-ion plasmas, Ind. J. Phys. **86**, 413 (2012).

[31] Note that it is possible to generate a stationary soliton by appropriate choice of F_1 instead, though the resulting coefficients will be different.

[32] A few terms were simplified using Kronecker δ's in Appendixes E and F. For instance, substituting the dimensional expressions into $\mathcal{G}'$ generates an ϵ^{-q} term multiplying σ_Q and an ϵ^{-p} term multiplying η and ζ. However, these can be neglected: as mentioned at the end of Appendix B, σ_Q carries an implicit $\delta_{q,0}$ while η and ζ have implicit $\delta_{q,0}$ and $\delta_{q,0}O(\zeta)/O(\eta)$, respectively. Similarly, the thermodynamic contribution of $\mathcal{F}'$ has a factor of ϵ^{-m^2}; however, given the presence of the Kronecker δ's, this is equivalent to ϵ^{-1}.

[33] Actually, as written, the coefficients in Appendixes E and F have all had a common factor of $\epsilon^{p/2-q/2}\sqrt{O(\sigma_Q)/O(\eta)}$ removed for brevity.

[34] Hence, c_1 is the normalized, order-unity analog of $n_{\rm max}$.

[35] D. Svintsov, V. Vyurkov, S. Yurchenko, T. Otsuji, and V. Ryzhii, Hydrodynamic model for electron-hole plasma in graphene, J. Appl. Phys. **111**, 083715 (2012).

[36] The sign of the β^2 term multiplying $u\partial_x u$ in Eq. (16) of [Ref. [15] should be flipped. Additionally, the expression for $F(v)$ in Eq. (26) should read

$$F(v) = \tilde{s}_0^2 - \frac{\beta^2}{2} - \frac{\beta_0^2}{1+v} - \frac{\beta_0^2\beta^2}{(1+v)^2}\frac{5-6\xi}{1-\beta^2} + \frac{v\beta_0^2(3-4\xi)}{(1+v)^2}. \tag{F14}$$

In the KdV equation, Eq. (27), the coefficient of the $v\partial_\zeta v$ term should be

$$(1-\xi)\left(2\tilde{s}_0^2 - \tfrac{4}{3}\xi + 4\beta_0^2\right). \tag{F15}$$

Also, the solution to the KdV equation, Eq. (28), should be

$$\delta n(z) = \delta n_{\rm max}\cosh^{-2}\left[\frac{z}{2}\sqrt{\frac{\mathbf{2}}{d_1 d_2}\frac{s_0^2}{2s_0^2 - v_F^2}\frac{\delta n_{\rm max}}{n_0}}\right], \tag{F16}$$

with Eq. (29) changed to

$$\delta n_{\rm max} = \mathbf{3}\frac{n_0}{2}\frac{u_0^2 - s_0^2}{s_0^2}, \tag{F17}$$

with corrections highlighted in bold. For the $u_0 \neq 0$ case, Eq. (34) should be adjusted by flipping the sign of the γ term multiplying the $u_0 \partial_x \delta u$ term. Furthermore, the dispersion relation, Eq. (36), should read

$$s_\pm = \frac{u_0(2-2\xi_0+\gamma) \pm \sqrt{s_0^2(1+\gamma) + u_0^2\left[(2-2\xi_0+\gamma)^2 - (1+\gamma)\left(3-\frac{10}{3}\xi_0+\gamma\right)\right]}}{1+\gamma}. \tag{F18}$$

[37] Note that Svintsov *et al.* [15] include factors of γ in the definitions of ε and n; here, they have been factored out to match our definitions.

[38] Note that Akbari-Moghanjoughi [14] uses a different terminology. There, the term "Dirac fluid" refers to massless fermions (as in graphene) while "Fermi liquid" refers to massive fermions. Both of these are dealt with in the completely degenerate $T = 0$ limit. By contrast, we follow the terminology of Lucas and Fong [1] to analyze both a "Fermi liquid" ($k_B T \ll \mu$) and a "Dirac fluid" ($\mu \ll k_B T$) regime for massless fermions. Therefore, the "Dirac" results in Akbari-Moghanjoughi [14] correspond to our $T = 0$ Fermi regime, while the "Fermi" results correspond to massive fermions not discussed here. Interestingly, bilayer graphene can induce such an effective mass for the quasiparticle excitations [61].

[39] Here we used the fact that $\mathrm{sgn}(\mathcal{A}'\mathcal{C}') = \mathrm{sgn}(v_0)$ for $u_0 = 0$.

[40] Note that this expression has a removable singularity at $u_0 = 0$; however, the double-sided limit exists and is 0.

[41] A number of other minor differences exist between our work and that of Akbari-Moghanjoughi [14]: there, velocities were normalized by c, giving $v_c = c/\sqrt{d}$. However, we found it more useful to normalize by v_F—yielding $v_c = v_F/\sqrt{d}$. This difference arose because Akbari-Moghanjoughi [14] chose to define $u^\mu = (c, \mathbf{u})/\sqrt{1-(u/c)^2}$ following Zhu and Ji [62], while we defined $u^\mu = (v_F, \mathbf{u})/\sqrt{1-(u/v_F)^2}$. Again, the choice of v_F, as opposed to c, is preferred since it preserves the form of the dispersion relation. Replacing the original choice of u^μ (involving c) with our choice (involving v_F) in Akbari-Moghanjoughi's derivation yields $v_c = v_F/\sqrt{d}$, i.e., our minimum propagation speed.

Finally, our expressions for the pressure differ slightly: it appears Akbari-Moghanjoughi [14] considered only $g = 2$ spin degeneracy in Eq. (4), rather than graphene's $g = 4$ spin/valley degeneracy. This only affects the normalization constant A_2 or A_3 in, for example, Eq. (11), and the subsequent conclusions are unaffected.

[42] This can be seen by noting that the expression is positive for $u_0 = 0$ and only crosses zero at ± 1, $\pm\sqrt{1+\lambda d}$, or $\pm\sqrt{1+\lambda d}/\sqrt{1+\lambda}$, with $\lambda := An_0^2/P_0(d+1)$. These are each greater than (or equal to) unity for $d \geqslant 1$; therefore, the entire expression is non-negative for $|u_0| \leqslant 1$.

[43] The $\mu_0 n_0$ term is non-negative because $\mathrm{sgn}\,\mu_0 = \mathrm{sgn}\, n_0$; cf., Eq. (Dirac:C2).

[44] Note that we have added an additional factor to the σ_Q term in order to account for the electrostatic interactions.

[45] A. P. Dmitriev, V. Y. Kachorovskii, and M. S. Shur, Plasma wave instability in gated collisionless two-dimensional electron gas, Appl. Phys. Lett. **79**, 922 (2001).

[46] V. N. Popov, Low-temperature specific heat of nanotube systems, Phys. Rev. B **66**, 153408 (2002).

[47] H. Bong, S. B. Jo, B. Kang, S. K. Lee, H. H. Kim, S. G. Lee, and K. Cho, Graphene growth under knudsen molecular flow on a confined catalytic metal coil, Nanoscale **7**, 1314 (2015).

[48] M. J. Ablowitz, D. J. Kaup, A. C. Newell, and H. Segur, The inverse scattering transform-fourier analysis for nonlinear problems, Stud. Appl. Math. **53**, 249 (1974).

[49] C. S. Gardner, J. M. Greene, M. D. Kruskal, and R. M. Miura, Method for Solving the Korteweg-Devries Equation, Phys. Rev. Lett. **19**, 1095 (1967).

[50] E. I. Kiselev and J. Schmalian, Boundary conditions of viscous electron flow, Phys. Rev. B **99**, 035430 (2019).

[51] R. C. V. Coelho, M. Mendoza, M. M. Doria, and H. J. Herrmann, Kelvin-helmholtz instability of the dirac fluid of charge carriers on graphene, Phys. Rev. B **96**, 184307 (2017).

[52] M. a division of Waterloo Maple Inc., Maple (2018), Waterloo, Ontario.

[53] D. Wood, *The Computation of Polylogarithms*, Tech. Rep. 15-92* (Computing Laboratory, University of Kent, Canterbury, UK, 1992).

[54] A. Lucas, J. Crossno, K. C. Fong, P. Kim, and S. Sachdev, Transport in inhomogeneous quantum critical fluids and in the Dirac fluid in graphene, Phys. Rev. B **93**, 075426 (2016).

[55] Note that one combination of parameters is not allowed in this derivation: $m < -1$ and $q = 0$. Due to the thermodynamic relations, $m < -1$ implies that T_1 will depend on density and pressure of the form $n_{1+|m|}$ and $P_{1+|m|}$. We are able to manipulate the results for $m = -1$ (cf., Appendix C 4) to handle these n_2 and P_2 terms. However, for $m < -1$ these terms cannot be eliminated. If $q > 0$, then μ_1 and T_1 do not appear in our first-order corrections, so this is acceptable; if $q = 0$, we would have these $n_{1+|m|}$ and $P_{1+|m|}$ terms, which cannot be eliminated.

[56] Furthermore, $m < -1$ precludes the choice of $q = 0$; see Ref. [55].

[57] Note that the expression for σ_Q in the Fermi regime lacks numerical factors; see Müller *et al.* [63] for the exact expression for the (screened) Fermi case.

[58] Equivalently, Lucas *et al.* [54] prove $P(\mu, T)$ only involves even powers by recognizing that the equation of state is charge-conjugation-invariant.

[59] Note that it is possible to generate a stationary soliton by appropriate choice of F_1 or F_3 instead, though the resulting coefficients will be different.

[60] M. Freitag, H.-Y. Chiu, M. Steiner, V. Perebeinos, and P. Avouris, Thermal infrared emission from biased graphene, Nat. Nanotech. **5**, 497 (2010).

[61] E. McCann and V. I. Fal'ko, Landau-Level Degeneracy and Quantum Hall Effect in a Graphite Bilayer, Phys. Rev. Lett. **96**, 086805 (2006).

[62] J. Zhu and P. Ji, Relativistic quantum corrections to laser Wakefield acceleration, Phys. Rev. E **81**, 036406 (2010).

[63] M. Müller, L. Fritz, and S. Sachdev, Quantum-critical relativistic magnetotransport in graphene, Phys. Rev. B **78**, 115406 (2008).